iScience

CellPress
OPEN ACCESS

Article

A systematic analysis of the costs and environmental impacts of critical materials recovery from hybrid electric vehicle batteries in the U.S.

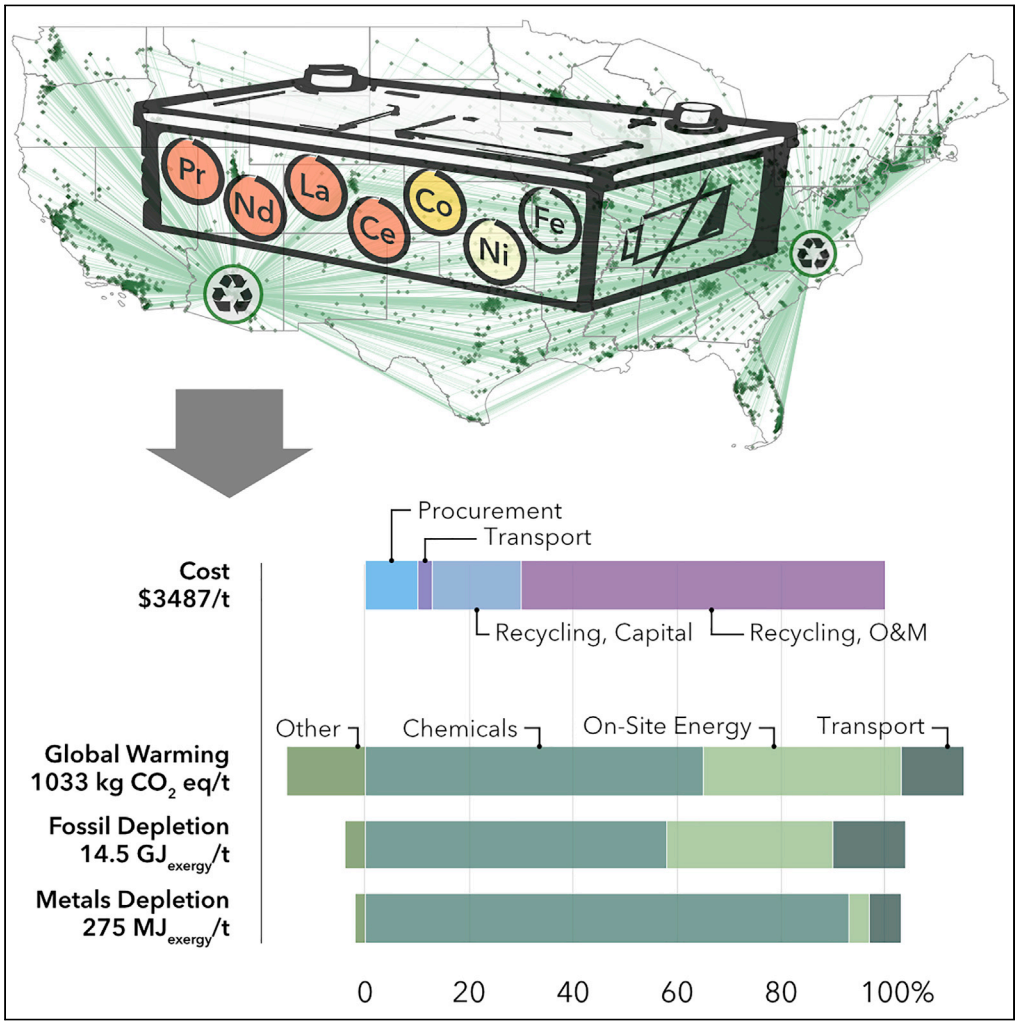

Chukwunwike O. Iloeje, Alinson Santos Xavier, Diane Graziano, John Atkins, Kyle Sun, Joe Cresko, Sarang D. Supekar

ciloeje@anl.gov (C.O.I.)
axavier@anl.gov (A.S.X.)
ssupekar@anl.gov (S.D.S.)

Highlights

We assess techno-economic and life-cycle impacts of large-scale HEV battery recycling

Recycling offsets primary critical material demand with lower environmental impacts

Flexible strategies mitigate investment risk from uncertain future battery availability

Marginal cost analysis can inform strategies for incentivizing collection and recycling

Iloeje et al., iScience 25, 104830
September 16, 2022 © 2022 The Author(s).
https://doi.org/10.1016/j.isci.2022.104830

iScience

CellPress
OPEN ACCESS

Article

A systematic analysis of the costs and environmental impacts of critical materials recovery from hybrid electric vehicle batteries in the U.S.

Chukwunwike O. Iloeje,[1,5,*] Alinson Santos Xavier,[1,*] Diane Graziano,[2] John Atkins,[1,4] Kyle Sun,[1,4] Joe Cresko,[3] and Sarang D. Supekar[1,*]

SUMMARY

Critical materials such as rare earth underpin technologies needed for a decarbonized global economy. Recycling can mitigate the supply risks created by the increasing demand and net import dependence, and enable a circular economy for critical materials. In this study, we analyze the feasibility and life-cycle impacts of recovering critical materials from spent nickel metal hydride batteries from hybrid electric vehicles in the U.S., accounting for stocks, battery scrappage, and end-of-life reverse logistics, given uncertain future availability scenarios. Our results show that the total collection and recycling costs depend strongly on future battery availability, with marginal costs exceeding marginal revenues when the availability of spent batteries declines. We quantify the potential of recycling to reduce primary imports, as well as the accompanying climate change and resource impacts. We explore the underlying reverse logistics infrastructure required for battery recycling and evaluate strategies for reducing associated capital investment risk.

INTRODUCTION

Critical materials are non-fuel abiotic mineral resources with vital economic importance, whose supply is considered to be at risk of disruption owing to any amount of geological, technological, geopolitical, environmental, and institutional factors (Graedel et al., 2015; Poulton et al., 2013). Critical materials have gained increased attention globally (Watari et al., 2020) and, in the U.S. (Biden 2021), owing to the vital technological functions they play in a broad range of low-carbon technologies. In 2021, the U.S. Department of Interior published a list of critical materials (see Table S1), based on an in-depth, interagency study, considering the materials' geographic concentration, their U.S. net import reliance, their recovery as byproducts from mining other minerals, along with other risk factors. Of the 50 minerals or mineral groups in the list, 33 are used in energy applications, including electric vehicles, light-weighting alloys, solar photovoltaics, and wind turbines that are pivotal to achieving U.S. decarbonization goals. Figure 1 shows a select few of these cleaner energy-critical materials. Rare earth elements (REE) stand out prominently on this list owing to a 100% import reliance, primarily on China, where the vast majority of the world's REE reserves and refining facilities are concentrated (Riddle et al., 2021). Despite its vast REE mineral resources, the U.S. has limited operational refining capacity, leading to the dependency of U.S. manufacturers on foreign supplies. This dependence creates supply vulnerabilities that jeopardize the U.S.'s energy decarbonization and circular economy goals.

To make the nation's REE supply chains more resilient, the U.S. Department of Energy has articulated three strategic pillars (U.S. Department of Energy 2021) — supply diversification, development of material substitutes, and reuse and recycling. In this paper, we focus on the recycling pillar; specifically, we examine EOL of spent NiMH batteries from HEV as a secondary source of U.S. domestic REE production. NiMH batteries in HEVs are a good candidate for recycling, as they contain REEs including neodymium (Nd), praseodymium (Pr), cerium (Ce), and lanthanum (La), and critical materials important to lithium-ion battery cathode production, such as nickel, (Ni), and small amounts of cobalt (DOE-EERE 2020; Ebin et al. 2018; Fetcenko et al., 2007). Moreover, hundreds of thousands of NiMH battery-powered HEVs introduced in the U.S. fleet circa 2000 are nearing their retirement, thereby potentially providing a reliable secondary source of these materials.

[1]Energy Systems Division, Argonne National Laboratory, Lemont, IL 60439, USA

[2]Decision and Infrastructure Sciences Division, Argonne National Laboratory, Lemont, IL 60439, USA

[3]Advanced Manufacturing Office, U.S. Department of Energy, Washington, DC 20585, USA

[4]These authors contributed equally

[5]Lead contact

*Correspondence: ciloeje@anl.gov (C.O.I.), axavier@anl.gov (A.S.X.), ssupekar@anl.gov (S.D.S.)

https://doi.org/10.1016/j.isci.2022.104830

This is an open access article under the CC BY-NC-ND license (http://creativecommons.org/licenses/by-nc-nd/4.0/).

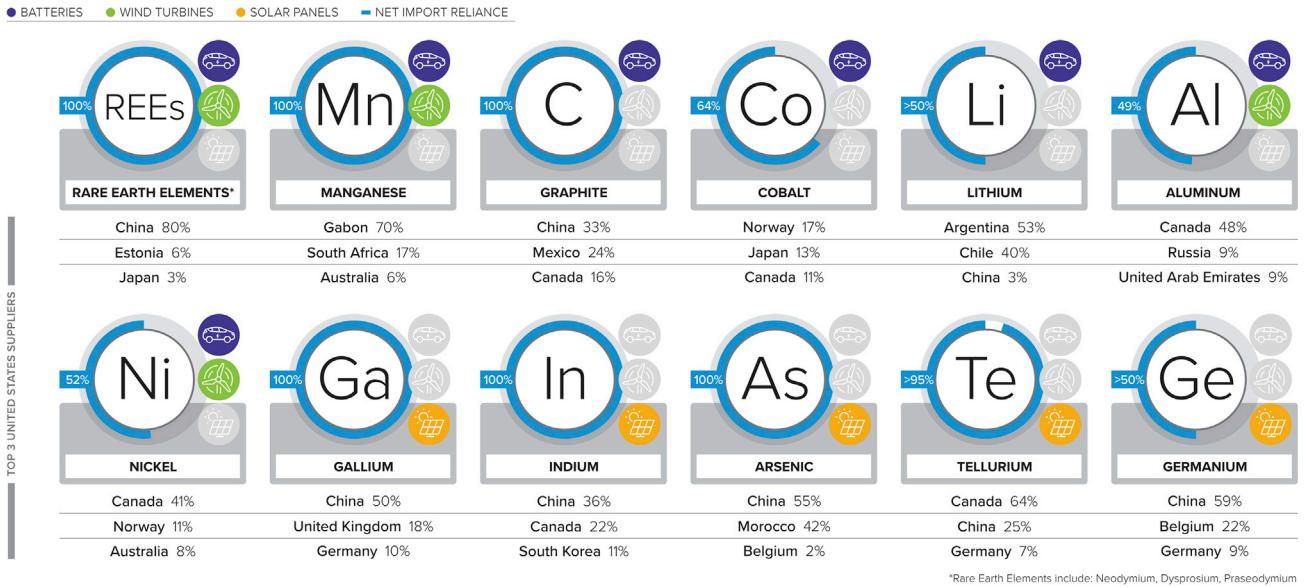

Figure 1. List of select critical materials essential to low-carbon energy technologies, shown with the U.S.' net import reliance and top 3 suppliers for each material

Data obtained from the 2020 U.S. Geological Survey mineral commodity summaries (U.S. Geological Survey 2020a).

Spent NiMH batteries are a potentially good source of critical rare-earth minerals. Unlike the recovery of nickel-iron (Ni-Fe/Fe-Ni) metals, which is already relatively advanced in the context of steel applications, the commercial recovery of REE is more nascent (Gaines 2014). Methods for REE recovery generally involve mechanical, hydrometallurgical, and pyrochemical processes (Innocenzi et al., 2017). Some recovery processes reported in the literature include mechanical separation to isolate battery electrodes, followed by acid leaching, selective precipitation, and, in some studies, solvent extraction (Ahn et al., 2020; Jha et al., 2022; Korkmaz et al., 2020; Zhi et al., 2021); bioleaching with organic acids at low temperature (Marins et al., 2020, 2022; Rasoulnia et al., 2021; Marins et al., 2022); high-temperature oxidation-reduction processes (Maroufi et al., 2018); mechanical pretreatment (Al-Thyabat et al., 2013; Ebin et al. 2018; Pinheiro et al., 2021); and synergistic co-recycling of NiMH and LiB (Liu et al., 2019; Rinne et al., 2021). Developing large-scale recycling for the U.S. needs detailed techno-economic analysis that extends beyond the boundaries of the processing facility to resolve uncertainty about associated costs. This study builds from the modeling and techno-economics of a hydrometallurgical process for recovering REE from NiMH batteries (Iloeje et al., 2019, 2020).

As the recycling process is anticipated to have significant impacts on the environment, an analysis of secondary recovery must also include a detailed environmental impact assessment. Whereas life-cycle assessments (LCAs) can elucidate the environmental impacts of NiMH battery production, use, and recycling, only a few studies have assessed the environmental impact of NiMH battery recycling. In an early study, Yu et al. (2014) evaluated the environmental impact of NiMH recycling (as measured by the Eco-indicator 99 system) and found the impact of recycling less than for incineration. More recently, Silvestri et al. (2020) evaluate the life-cycle impacts of recycling NiMH vehicle batteries associated with the European Union's collection and recycling targets (European Union, 2020; Melin et al., 2021). The authors find that environmental impacts decrease when recovered materials (specifically, iron, mixed RE metals, and nickel) replace their associated virgin materials in NiMH battery manufacturing. Wang et al. (2021) report on an LCA and sensitivity analysis of reuse, recycling, and disposal both of a single and fleet of spent NiMH vehicle batteries in Japan. The authors find that CO_2 emissions, non-renewable energy demand, and resource depletion are highest for the recycling-only case and least for the no-recycling case. In their study, the no recycling case assumes consumption of primary metals and not those recovered from recycling. Rinne et al. (2021) conducted an LCA based on simulated results of an experimental co-recycling process for NiMH and lithium-ion batteries. Their analysis indicates the possibility of reduced climate change, acidification, human toxicity, and freshwater eutrophication from the recycling process compared with primary production. The authors accredit the majority of these reductions displacement of primary production of nickel and cobalt sulfates. By

linking LCA analysis with an optimized reverse logistics, our study adds an important perspective on the environmental impact of closed-loop recycling and recovery of rare earth metals from EOL HEVs in the U.S.

Circular economy mandates and corporate responsibility expectations have intensified the importance of sustainably managing EOL products (Agrawal et al., 2015; Govindan and Soleimani, 2017; He et al., 2020; Islam and Huda, 2018; Ni et al., 2021; Salim et al., 2019). Several studies have evaluated the reverse logistics of EOL vehicle batteries, most recently for lithium-ion batteries (see e.g. Akram et al., 2021; Azadnia et al. 2021). Whereas the optimization methods and objective functions applied in such studies vary, they are mostly, if not all, regionally specific by country or region [e.g., China (Wang et al., 2020a), India (Kannan et al., 2010), Sweden (Tadaros et al., 2020), Turkey (Demirel et al., 2016), and California (Hendrickson et al., 2015)]. Our study extends these analyses by integrating reverse logistics optimization with a physics-based techno-economic analysis of NiMH battery recycling at a relevant scale to inform policy development. Whereas the focus of this study is the U.S., the analytical methods are applicable to other regions and for other types of EOL products.

A key contribution of this study is a robust, system-level assessment of battery recycling that extends the analysis boundary beyond the unit process to account for stocks, time-resolved availability, and the logistics of procuring spent NiMH batteries in the U.S. context. This broader strategy goes beyond simpler estimates to identify the impact of resource distribution and location-based cost factors on cost-optimized plant locations, sizes, and overall recycling costs. In addition, it provides insight into how the evolution of spent battery availability affects capacity utilization and investment risk, as well as the ability of recycling to offset imports and reduce critical material supply risk. In this paper, we estimate the material flows, costs, energy use, greenhouse gas (GHG) emissions, and material depletion associated with the recovery and recycling of spent NiMH batteries in the U.S. Our results identify key cost and risk drivers, and examine strategies to mitigate the investment risk associated with uncertain future battery availability. We show the extent to which NiMH battery recycling could substitute critical material imports, evaluate environmental impacts relative to primary production. We conclude with recommendations to promote recycling and improve critical material supply resilience.

RESULTS

Availability of spent NiMH batteries

The design of the recycling network critically depends on the future amount of spent NiMH batteries available annually for recycling across the U.S. As these projections are not readily available, we estimate them using a stock and flow model of HEVs on historic HEV sales data (Gohlke and Zhou, 2020) from 2000 to 2021, HEV sales projections through 2050, extrapolating from historic sales data, HEV battery technology by vehicle model (Davis and Gary Boundy, 2021), and a logistic vehicle scrappage probability function (Supekar and Skerlos, 2017). HEV sales were projected to increase monotonically following historical trends from Gohlke and Zhou (2020). We consider two possible future scenarios for HEV sales projections to provide lower and upper bound estimates for spent NiMH batteries available for recycling. A "conservative" scenario projects a decline (modeled as a sigmoid function) in the proportion of NiMH batteries in HEVs characterized owing to substitution by Li-ion batteries following recent historical trends. The "optimistic" scenario assumes that the proportion of NiMH batteries in HEVs will stay constant in future years. Future sales of NiMH HEVs under both scenarios were obtained by multiplying projected annual total HEV sales with the fraction of NiMH batteries in both scenarios. The number of spent batteries generated each year was then estimated by applying a vehicle scrappage probability function to the annual sales data (see STAR Methods for mathematical formulations of stock and flow model). Reports from accelerated battery testing (Bernard and Lippert, 2015) and field data (O'Dell, 2014; Tatarevic, 2016; Motorcells Hybrid Battery Renewal & Installation, 2018) suggest that most NiMH batteries last the lifespan of an HEV ranging from 150,000 to 200,000 miles, and as such the scrappage rate of NiMH batteries in this study is assumed to be the same as the scrappage rate of HEVs.

Options for spent vehicle batteries include recycling, repurposing, remanufacturing, and disposal (Rajaeifar et al., 2022). In the absence of a systematic study on the rates or likelihood of the different EOL fates of HEV NiMH batteries, we assume in this study that only 50% would be available for recycling. This number is assumed to include collection efficiency and losses to other fates. As a comparator, the European Union has recently issued a policy target for lithium-ion battery recycling of 65% by 2025 and 70% by 2030, though no specific targets promulgated for NiMH battery recycling (European Union, 2020; Melin et al., 2021). We

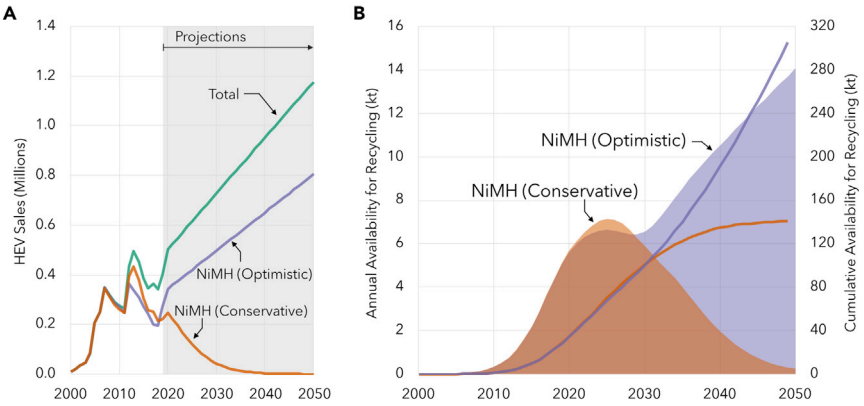

Figure 2. HEV sales and scrappage projections

(A) U.S. HEV historic sales and future projections under conservative and optimistic scenarios for the fraction of total HEVs containing NiMH batteries.

(B) Annual (shaded areas) and cumulative (lines) projections of mass of spent NiMH batteries available for recycling.

estimate the average weight of an NiMH HEV battery at 46 kg based on battery specifications from various sources (Castro, 2016; Davis and Gary Boundy, 2021; Kelleher Environmental, Gracestone, Inc., and Millette Environmental, 2019; Young et al., 2013). Based on these modeling data and assumptions, the annual sales of HEV with NiMH batteries are shown in Figure 2A, and the estimated mass of spent NiMH batteries available for recycling is shown in Figure 2B for both conservative and optimistic scenarios for future NiMH HEV sales.

Materials flows in NiMH battery recycling

The distribution of recovered material flows from recycling is important for understanding the relative economic potential of the recovered material streams, especially in the context of their respective markets. Consequently, we next determine the material flow balance and the distribution of recovered materials from spent NiMH battery recycling. Central to this analysis is the recovery of didymium metal (neodymium-praseodymium/Nd-Pr) from the spent NiMH batteries, as well as high-grade Nickel metal. Other significant battery material-derived flows include cerium-lanthanum (Ce-La), mixed hydroxides (e.g., $Co(OH_2)$, $Ni(OH_2)$), and mixed metal scraps (Ni-Fe, Fe-Ni), as well as those set for landfill or other disposal – salts, leach residue, and plastics. The recycling process includes battery disassembly (battery is assumed to enter the facility in a discharged state), followed by anode and cathode recycling in separate physical and hydrometallurgical sub-processes, and finally solvent extraction following the anode recycling sub-process to separate the REEs. The disassembly, physical and hydrometallurgical separation processes are based on Sabatini et al. (1994b), in which hydrochloric acid is used as a leaching agent. The solvent extraction process is based on the REE recovery process described in Iloeje et al. (2019). Figure 3 provides an overview of the material flows through the recycling process and the potential economic value of the various recovered products at their current market value (see Table S10).

Didymium metal and high-grade Nickel metal are the two most valuable co-products of the recycling process based on revenue potential, on a per unit mass basis. Other economically significant co-products include battery-grade mischmetal, Ce-La alloy (roughly 20/80 mix), hydroxides of Co, La, Mn, Al, Ni, and other metals, and mixed metal scraps (Ni-Fe, Fe-Ni). Although didymium accounts for <1% by mass of the total recovered materials, it accounts for over 14% of the total potential revenue from all recovered products. Similarly, Ni accounts for about 5% by mass of the total recovered products but makes up over 36% of the total potential revenue. Whereas Ni-Fe and Fe-Ni scraps represent a large proportion of the outputs by mass (27%) and potential revenue (38%), revenue recovery from scrap markets is uncertain because of the oversupply of recycled scrap from EOL automobiles, structural steel, appliances, rebar and reinforcement steel, and steel packaging, whose current recycling in the U.S. range from 70 to 100%(Tuck, 2020). The two major waste streams – salts and plastic from casing – account for over 50% of total flows.

Potential for displacing primary materials demand

Based on the developed battery availability scenarios and material flow distributions, we estimate the potential of the recovered critical nickel and rare earth metals to displace primary demand. Figure 4

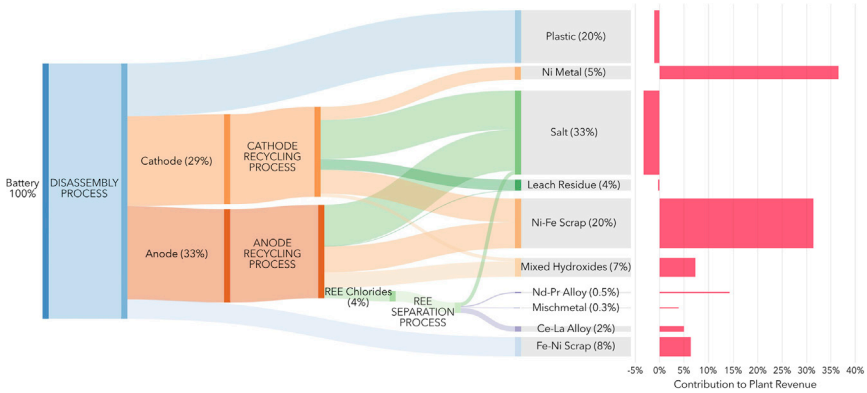

Figure 3. Sankey diagram on the left showing mass fractions (in parentheses) of product flows in the battery recycling process and the potential revenue fraction of recovered products (pink) on the right assuming all recovered materials are sold

Negative revenue indicates disposal costs of waste products. Value of REE products and Ni metal based on an expected purity of 99% or higher, based on the hydrometallurgical separation process used in this study.

shows the potential of recovered products from the NiMH recycling complex to displace the didymium and nickel contained in NiMH batteries in HEVs in the U.S. In the conservative scenario (Figure 4A), didymium and nickel recoveries exceed the demand for didymium and nickel from new HEVs for most years. In the optimistic scenario (Figure 4B), however, didymium and nickel recovery rates are found to be significantly lower than the demand for those materials from new HEVs owing to the increasing sales of NiMH HEVs with time in this scenario. Didymium has a higher recovery rate than nickel in both scenarios because nickel flows in the recycling process bifurcate into pure Ni and Ni-Fe/Fe-Ni scrap streams as shown in Figure 3. The potential for displacing primary battery grade nickel is therefore lower than the potential for displacing primary didymium.

Relative to recent total U.S. demands for didymium [<160 tonnes per year or tpy; (Castilloux, 2016) and primary nickel (~100,000 tpy (McRae, 2021)], a different story emerges. In neither of the scenarios examined in this study would the recycling complex provide nearly enough product to meet U.S. demand. Yet, given that the U.S. currently has negligible primary production of these metals, recycled didymium and nickel should be marketable. In the case of didymium, recycling could potentially provide feedstock in the case that sintered NdFeB magnet production is resumed in North Carolina (Lombardo, 2020). With a reported capacity of 2,000-tpy NdFeB and assuming 30% didymium content, demand for the didymium alloy for such a plant would be on the order of 600 tpy. In this case, NiMH battery recycling in the optimistic scenario for NiMH HEV future sales could meet approximately 8–16% of the magnet facility's didymium demand.

The analysis illustrates the challenges associated with recovering critical materials from EOL products. In finished products, the weight percent of critical materials is often low, and as in the case of NiMH batteries, significant equipment and processing are required to isolate and purify them into saleable products. More importantly, both the future feedstock volume and composition are highly uncertain, with substitution potential strongly dependent on which future evolves. Therefore, to achieve supply resilience as well as circular economy objectives, these challenges need to be overcome. Options for advancing the recovery of REEs from NiMH batteries might include (1) co-recovery and processing of consumer and vehicle NiMH batteries; (2) established agreements to separate the REEs in equipment at primary mines (e.g., Mountain Pass in the U.S.); or (3) increased recycling rate via policy options requiring manufacturers to take ownership of EOL products, as well as incentives to pursue circular economy approaches. Unconventional sources are another option for REE recovery, though the REEs are present at low concentrations in these potential feeds. As a point of perspective, recovery of didymium from 500,000 tonnes/year of Appalachian coal ash could provide about 20 tonnes/yr (Jin et al., 2017). In summary, given the importance of REEs to U.S. and global decarbonization goals and the majority of countries' current net import reliance on their supply, all options should be considered for increasing their supply resilience.

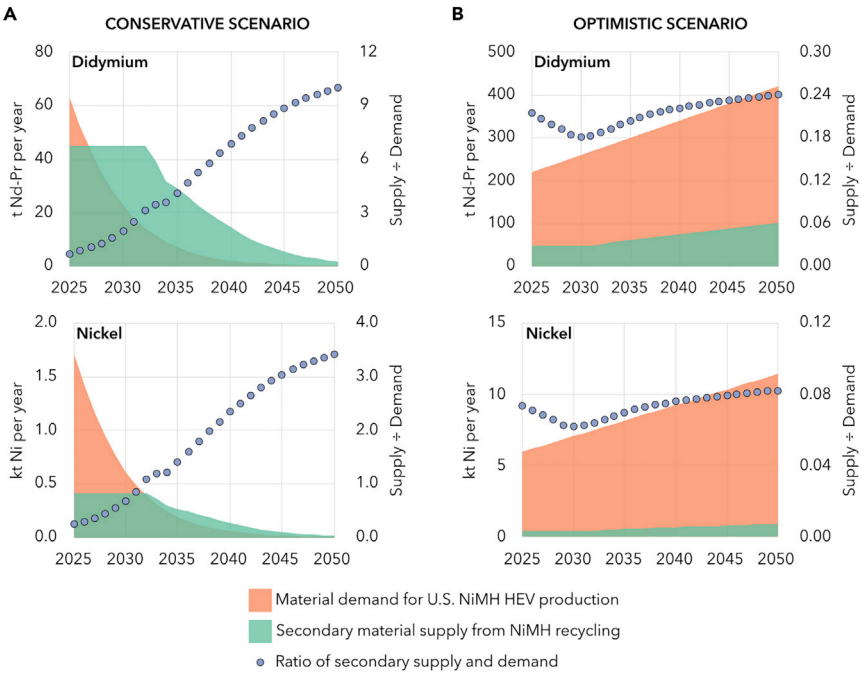

Figure 4. Target critical material substitution potential

Didymium and nickel embedded in HEV NiMH batteries sold in the U.S. that could potentially be displaced by didymium and nickel recovered from the NiMH recycling in the (A) conservative scenario and (B) and optimistic scenario.

Reverse logistics network infrastructure and costs

A robust evaluation of the techno-economics of prospective NiMH battery recycling in the U.S. requires estimates of infrastructure, collection and transport logistics costs. Accurately estimating infrastructure and logistics costs, however, requires determining the number of recycling facilities, as well as their capacity and geographical location. *Optimal* locations and capacities of the recycling facilities to process the spent NiMH batteries were determined using RELOG (Xavier et al., 2020), a supply chain software package developed at Argonne National Laboratory which employs mixed-integer linear optimization to find the reverse logistics network that minimizes the total cost of collecting, storing and recycling EOL products. It includes costs for transportation and warehousing, as well as capital costs (new plant construction and capacity addition) and operating costs (including labor, energy, materials, and waste disposal) of the recycling process (see Tables S2–S7 for cost data). The sizing and deployment of recycling facilities are based on the annual spent NiMH battery flows shown in Figure 2B during the 2025–2050 period. Figure 5 shows the cost-optimized reverse logistics network, costs, and key cost contributors for NiMH battery collection and recycling across the continental U.S.

The analysis shows that the reverse logistics network for NiMH battery recycling favors large, centralized facilities that exploit economies of scale. This result is consistent with the findings of Lander et al. (2021) in their analysis of the economic viability of battery recycling plants, in which they show that the recycling cost sharply decreases and profitability sharply improves beyond a certain threshold annual recycling capacity, although this effect yields diminishing returns beyond this threshold. The location results in Figures 5A and 5B realize a trade-off between proximity to high-density EOL battery sources — which determine transportation costs — and regional cost differences — which influence installation costs. For the conservative scenario shown in Figure 5A, our analysis identifies two major recycling facilities — one in Arizona processing about 62% of spent batteries and the other in North Carolina processing the remaining 38%. For the optimistic scenario shown in Figures 5B and 5A third plant is introduced to process higher volumes of spent batteries, with facilities in Arizona, Washington, and South Carolina processing about 43%, 20%, and 37% of the spent batteries, respectively. We note that the precise location of the recycling facility depends on several assumptions and constraints developed for this study, which are described in detail in the STAR Methods section. Notwithstanding the geospatial, economic, and regulatory factors and diverse decision-making possibilities of multiple

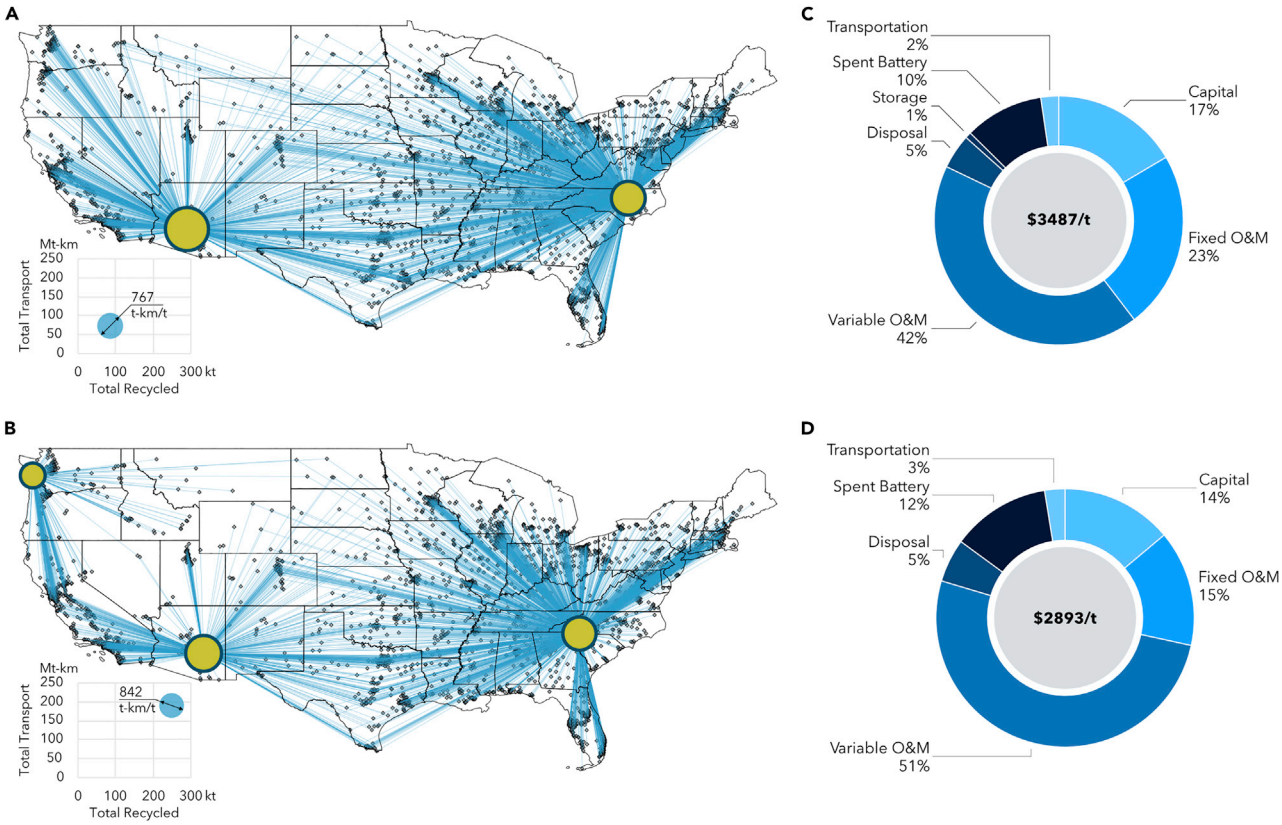

Figure 5. Cost-optimized reverse logistics network with breakdown of cost contributions

Cost-optimized recycling facility locations in the (A) conservative and (B) optimistic scenarios for the spent NiMH battery availability. Yellow circle sizes represent the size and locations of recycling plants and diamonds represent spent battery collection centers. Transportation routes between collection centers and recycling facilities are assumed to be straight-line approximations. Inset *x*–*y* plots below the maps in (A) and (B) show the total amount of spent NiMH batteries recycled and transported between 2025 and 2050 in the respective scenario. Levelized cost per unit of battery recycled along with cost breakdown in the (C) conservative and (D) optimistic scenarios for the spent NiMH battery availability.

agents that are beyond the scope of this work, the reverse logistics modeling and analysis in this study provides a more informed estimate of the transportation distances and costs of a nation-wide battery-recycling network than simple assumptions of average transportation distances elsewhere in the literature.

Figures 5C and 5D show the total cost per tonne of battery recycled, and breakdown of costs for the conservative and optimistic scenarios, respectively. The levelized cost of collecting and recycling NiMH battery is estimated to be about $3,500 and $2,900 per tonne for the conservative and optimistic scenarios, respectively. This range of cost compares fairly with estimates of hydrometallurgical LiB recycling costs in the literature, which range from $1,540–8,430 per tonne in an analysis by Thompson et al. (2021) (lower end of the range corresponds to inorganic acids and higher end corresponds to organic acids as leaching agents), $3,730 per tonne in a study by Qiao et al. (2019) on battery recycling in China, and $3,400 per tonne in a study by Xu et al. (2020) based on Argonne National Laboratory's EverBatt model (Dai et al., 2019).

Variable plant operating & maintenance costs, which include labor, material, battery acquisition, and energy expenditures per unit of battery recycled, are the largest contributors to the total cost – accounting for over 40% and 50% in the conservative and optimistic scenarios, respectively. Battery transportation and storage accounts for the smallest fraction of the total cost, contributing about 3% in both scenarios. The difference between the costs for the conservative and optimistic scenarios is primarily owing to the differences in average utilization (Figure S7A). As explained later, declining quantities of spent batteries in the conservative case leads to lower levels of recycling plant utilization.

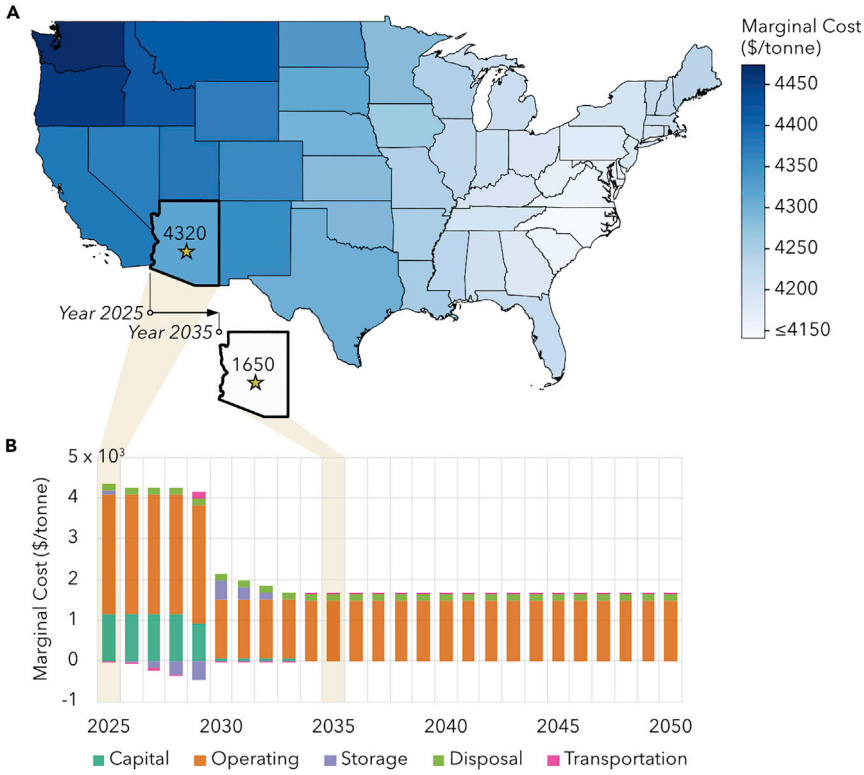

Figure 6. Locational marginal costs for NiMh battery recycling in the U.S.

(A) Location-specific marginal costs for the conservative battery availability scenario.

(B) Breakdown of marginal cost over time for a select collection center in Phoenix, Arizona, first shown in Figure 5A.

Whereas profitability analysis was not the focus of this study, a simple revenue/cost analysis at prevailing market rates shows that the revenue potential from the recovery of Ni and Didymium accounts for just 50%–60% of total recycling cost per battery (60%–70% including all rare earth products) for conservative and optimistic scenarios respectively. Therefore, profitability requires revenue recovery from all recycled product streams. Including all recovered streams results in revenue/cost ratios of about 105% and 130% for the conservative and optimistic cases respectively. However, realizing the full revenue potential could be tricky, particularly with the uncertain markets for Ni-Fe and Fe-Ni scrap metals as discussed earlier.

Marginal cost of NiMH battery recycling

Location-specific marginal costs shown in Figure 6 represent the additional cost to recycle a tonne of additional material from a given location. These costs are an important economic metric as they guide the behavior of profit-maximizing firms. Specifically, such firms would likely decide to process additional material only if the expected revenue from recycling it (including any subsidies) exceeds the marginal cost. Marginal costs can be computed by optimizing the supply chain network model with small increases in demand at a particular collection center, then comparing the solutions. We performed this marginal cost analysis in this study by fixing the optimal facility locations obtained in the baseline model scenario and allowing only decisions related to transportation, storage, and expansion to change.

This analysis shows that marginal costs for NiMH recycling depend strongly on a combination of multiple parameters, including maximum plant storage and the total amount of recycling feedstocks available over time. In general, marginal costs for collection centers located in the proximity of a recycling facility were lower than those for centers located farther away, indicating that some regions may require higher levels of subsidy/incentives to make recycling economically attractive. However, because marginal costs are dominated by expansion and operating costs and not by transportation costs, the regional variation is somewhat smaller than one would expect. Aside from proximity to recycling a facility, regional differences in installation costs, as well as whether or not the facilities are operating at full capacity also influence

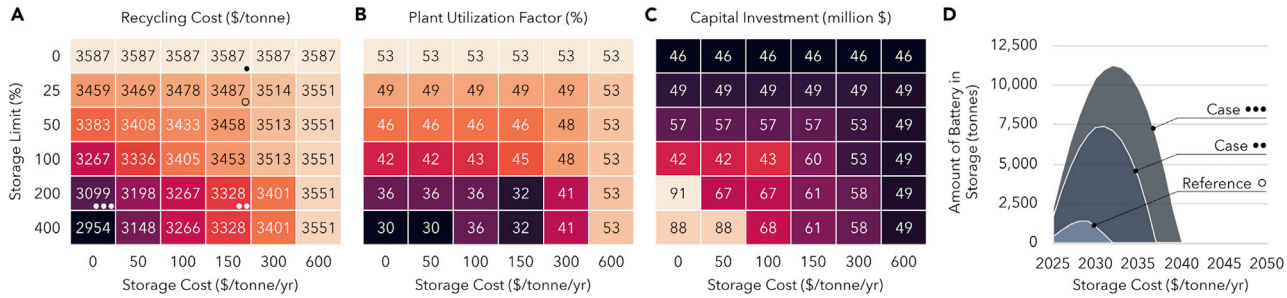

Figure 7. Sensitivity analysis on impact of varying storage limit and cost

Sensitivity analysis examining effects of the spent battery storage (warehousing) costs and capacity on (A) recycling costs, (B) plant utilization factors, and (C) capital investment costs. Darker shades indicate lower values. The box marked by ○ in the heatmap in (A) represents the storage limit and cost values used in the baseline analysis in this study. (D) Comparison of the total amount of spent batteries stored over time under various combinations of the storage limit and costs, as marked by ○, ●●, and ●●● in panel (A).

marginal costs; plants that have the slack capacity and can process additional material without expansion, which lowers marginal costs significantly. States on the East coast of the U.S., which have lower installation costs than other regions, have a lower marginal cost as shown in Figure 6A.

Marginal costs in the conservative scenario for spent NiMH battery availability are found to be considerably higher in the first few years of operation compared with latter years and are likely to exceed the expected marginal revenue. It is unlikely, therefore, that a profit-maximizing firm would decide to process all spent batteries available in the first years without additional incentives. Marginal costs in the initial years of operation of recycling facilities are in the range of $4,100–4,500/tonne, as shown in Figure 6B, and they are driven by variable operating (34%), fixed operating (33%), and expansion (23%) costs. Marginal costs drop considerably in later years of operation year to about $1,600–1,850/tonne as facilities cease to expand their capacity in the wake of the waning supply of spent batteries. In these later years, total marginal costs can be broken down into variable operating (85%), disposal (9%), and transportation (6%) marginal costs, and locational variations are caused exclusively by differences in transportation costs. Such spatiotemporal analyses can thus help in the planning of an informed strategy based on several "what-if" scenarios to incentivize battery collection and recycling investments in the U.S.

Mitigating the risk of uncertain future availability

If battery availability declines over time, plant utilization factors would fall (Figure S7), leading to higher per-tonne recycling costs and jeopardizing capital recovery. If facilities are built to immediately accommodate the high EOL battery flows expected from a fast-retiring fleet of HEVs, they may end up being oversized to handle reduced flows in later years from a waning technology. Thus, even though the first few years of operation of the recycling facility would result in high utilization factors from a combination of higher EOL battery flows and use of limited storage (up to 3 months' worth), production from the facility would drop in the future unless supplemented by waste products that could be handled by the same process. It must be pointed out here that the low utilization rates in the latter years are partly an artifact of the requirement in this work that all batteries available each year must either be recycled or stored, given the commitment to secure critical material supply. Removing this requirement could allow a better-utilized recycling infrastructure, even under declining EOL battery availability. Nevertheless, this scenario provides a measure of the risk to investors arising from uncertain battery availability, and the consequent facility underutilization.

Unlike in the conservative scenario, the optimistic scenario for the availability of spent NiMH batteries shows maximum utilization throughout the simulation window (see Figure S7A). This is because the quantity of batteries available for recycling would increase over time, requiring capacity expansion (see Figure S7B). The primary significance of these utilization trends is that besides economies of scale, facility locations, and transportation distances, the capacity utilization factor also drives the difference in recycling costs per tonne of battery processed between the optimistic and conservative scenarios examined in this study.

To mitigate capacity underutilization risks from a possible decline in battery availability, we explore the effectiveness of warehouse storage as a lever for improving recycling economics. Figure 7 summarizes the results of a sensitivity analysis in which we ran the logistics optimization model for various combinations

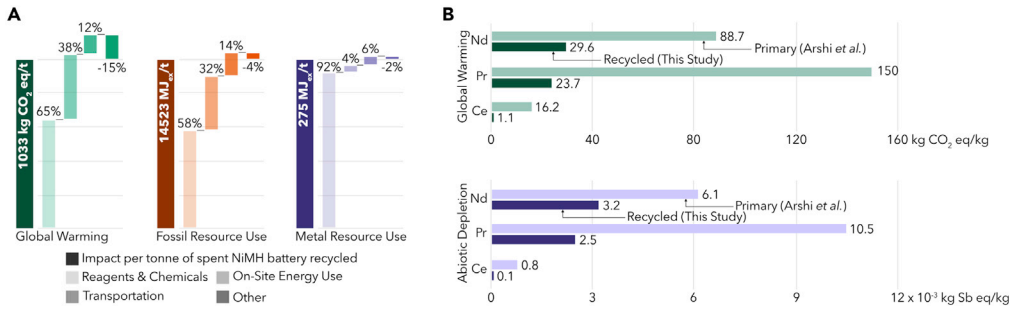

Figure 8. Life-cycle environmental impacts of NiMH battery recycling

(A) Life-cycle environmental impacts of collecting and recycling 1 tonne of spent batteries for the conservative scenario.
(B) Environmental impacts expressed per kg of select recovered rare earth metals, and their comparison with impacts of primary (virgin) extraction of those rare earth metals.

of warehouse storage limit (expressed as % of annual production capacity) and warehouse storage costs (expressed om $/tonne/year). Figure 7A shows that by increasing the storage limit, the cost of recycling a tonne of spent batteries would fall by about 7% in going from case ● to case ●● and by 14% in going from case ● to case ●●● if economies of scale in storage facility costs are assumed to be negligible. Increasing storage capacity improves overall facility utilization (Figure 7B), which ultimately allows smaller recycling plants to be built (Figure 7C). Figure 7D compares the annual storage for the baseline case ○ with cases ●● and ●●●. It shows that to realize the reductions in recycling costs suggested earlier, up to 5 times more batteries will have to be stored compared with the reference case used in this analysis.

The comparative analysis here suggests that investing in a reverse logistics infrastructure design that favors building larger storage facilities can mitigate the investment risk for a low battery availability future, with the potential to reduce the cost variation between the conservative and optimistic limits by at least 30% and up to 70%. As the specific cost of storage is lower than that for recycling capacity, it would be less expensive to oversize storage than to oversize the recycling facility. Moreover, warehouse storage is inherently multipurpose and can be repurposed to store other products to maintain a high utilization factor. Besides storage, other strategies such as designing flexible facilities to handle multiple feedstocks (e.g., other battery types), and co-location with primary processing facilities can augment utilization and limit investment risk.

Environmental impacts

The environmental impacts of spent NiMH battery collection and recycling are evaluated using an LCA framework based on the material and energy flows shown in Figure 3 and characterized in detail in Figure S1 and Table S11. Details of the LCA are provided in the STAR Methods section. Given the obvious climate–materials–energy intersection of the cleaner energy critical materials challenge driving this analysis, we focus our LCA on climate change and abiotic materials depletion impacts. Climate change impacts, expressed in kg CO_2 eq, are characterized based on the ILCD 2011(European Commission Joint Research Centre, 2012) impact assessment method. Abiotic material depletion impacts that are further broken down into fossil resource use and metal resource use and expressed in MJ of exergy stored in the resource, are characterized based on the Cumulative Exergy Demand (Bösch et al., 2006) impact assessment method. To facilitate comparison of our environmental impacts analysis with impacts of primary extraction published by Arshi et al., we also calculate the total abiotic depletion, which includes all fossil, mineral, metal, and bulk resources and is expressed in kg Sb eq, using the ILCD 2011 impact assessment method. Impacts are calculated per tonne of spent NiMH batteries recycled. Impacts per kg of economically useful product from the recycling process are also calculated using an economic allocation method, which ascribes the process impacts to the different products in direct proportion to the product's contribution to the total potential revenue (see STAR Methods for details). Figure 8 shows the results of the LCA analysis for the conservative scenario for spent battery availability. Results for the optimistic case are quite similar to the conservative case and are shown in Figure S2. Complete LCA results for both scenarios covering all environmental impact categories are shown in Tables S12–S15.

We find that collecting and recycling 1 tonne of spent NiMH batteries would lead to a global warming impact of 1,033 kg CO_2 eq, fossil resource use of 14,523 MJ_{ex}, and metal resource use of 275 MJ_{ex}, as shown

in Figure 8A. These impacts are largely driven by the use of chemicals and reagents in the recycling process. On-site electricity use is the second largest driver of global warming and fossil resource use. Negative contributions to total impacts in Figure 8A are owing to resource recovery and credit for displaced impacts from waste incineration. In contrast to the relatively small contribution of transportation to the system costs (see Figure 5), transportation of the spent batteries contributes to about 12% of the global warming and 14% of fossil resource use impacts. Compared with impacts of primary production from the Bayan Obo mine in China based on the analysis by Arshi et al.(ArshiPraneet et al., 2018), Figure 8B shows that recycled neodymium, praseodymium, and cerium have a 67%, 84%, and 93% lower global warming impact and 48%, 76%, and 85% lower abiotic depletion impact, respectively. This suggests that the use of recycled REEs from spent NiMH batteries would therefore not only increase domestic REE production, but also reduce the unit environmental impacts of REEs.

Our results compare well with other hydrometallurgical battery recycling estimates in the literature. The Ecoinvent (Ecoinvent Center, 2018) process for hydrometallurgical recycling of LiBs (no transportation), which assumes sulfuric acid as the leaching agent, has global warming impact of 904 kg CO_2 per tonne of spent battery compared with 909 kg CO_2 eq (excluding transportation) in this study. In a study on LiB recycling by Mohr et al. (2020), they find that the life-cycle global warming impact from hydrometallurgical recycling of LiBs (considering no displaced impacts from products) ranges between 4.07 and 6.47 kg CO_2 eq per kWh of storage capacity depending on the LiB chemistry. This range corresponds to a global warming impact of 661–1,021 kg CO_2 eq per tonne of spent battery when factoring in the energy density (Wh/kg) of the different battery chemistries.

Ciez and Whitacre (2019) conducted an LCA of recycled NiMH batteries based on the hydrometallurgical process described in the Argonne GREET model (Wang et al., 2020b), in which an organic acid is used as a leaching agent and hydrogen peroxide as a reducing agent. Their results, which include transportation, show a global warming impact of about 700–950 kg CO_2 eq/ per tonne of spent battery. The bench-scale hydrometallurgical process in GREET on which their analysis is based assumes a 90% acid recovery and reuse (Dunn et al., 2012), which significantly reduces reagent use and therefore reduces the life-cycle greenhouse gas emissions. Although our study assumes a 30% reduction in HCl consumption compared with Sabatini et al. (1994b), further reduction in acid use is possible via acid regeneration. However, such regeneration processes require additional chemicals such as sulfuric acid and consume additional energy (McKinley and Ghahreman, 2018), which would add to the environmental impacts and cost of the overall process. As such, a cost-benefit analysis of acid recovery measures is advised to ascertain its merits in reducing overall reagent use and environmental impacts of the battery recycling process.

DISCUSSION

The goal of decarbonizing the U.S. economy by 2050 requires a vast expansion in cleaner energy and transportation technologies including electric vehicles and wind turbines. This expansion is already driving up demand for raw materials critical to these technologies – materials for which the U.S. is heavily import-reliant on geopolitically sensitive regions of the world – creating supply risks for the U.S. Systematic recovery of these critical materials from spent hybrid vehicle NiMH batteries could partly offset reliance on imports, contribute to securing their long-term supply, and support the U.S.'s circular economy goals. In this study, we evaluated costs and broader impacts associated with a systematic large-scale NiMH battery-recycling complex, accounting for stocks, time-resolved availability, and the logistics of procuring the spent batteries.

Spent NiMH batteries could provide a reliable alternative source of recycled didymium and nickel, though their potential to displace the primary demand for these critical materials depends on how the proportion of NiMH batteries in HEVs evolves in the future. Given that the U.S. has limited to no capacity for producing refined rare earth and nickel metals, domestic recycling can offset some dependence on imports for the supply of these materials, with the potential to reduce both the political and environmental burdens of primary extraction of these materials. In terms of capacity to displace imports, the higher supply to demand ratios in the conservative scenario show complete displacement potential within the NiMH product market, and capacity to improve material supply security. The situation is reversed for the optimistic scenario owing to the time lag between demand and scrappage, which leads to a large mismatch between material recovery and material demand. With current vehicle battery chemistry trends, it is more likely that any recovered rare earth would go in as feedstock to other product markets such as permanent magnets.

Compared with their proportion of total material flow through the recycling process, rare earth metals and nickel account for a disproportionately high potential revenue from the sale of recycled products. Nickel-iron scrap represents the other potentially significant source of revenue from recycled material but given the current oversupply of scrap from other sources like structural steel and automobiles, their actual market value is uncertain. Whereas profitability analysis was not the focus of this study, these considerations suggest that the economics of NiMH recycling cannot solely depend on revenue from the rare earth and nickel recovery, but must include potential revenue from all other recovered products. In general, the recycling network structure results from a trade-off between transportation and plant construction costs, respectively determined by proximity to spent battery sources, and regional cost differences. Environmental impacts are largely driven by chemicals and reagents used in anode and cathode recycling and solvent extraction processes. Whereas the contribution of transportation to the unit cost of recycling a tonne of spent batteries is small, transportation contributes significantly to global warming and fossil resource depletion impacts. Electrified transportation can reduce mobility-related emissions impacts, whereas alternative technologies (e.g., acid-free leaching and solvent recovery) can mitigate impacts from reagent use.

EOL NiMH battery sources of rare earth could evolve to vastly different levels of availability by 2050. The estimates for the conservative and optimistic scenarios provide reasonable upper and lower bounds on the expected cost of battery recycling, and the difference between them reflects important contributions from the economy of scale and facility utilization. If the current trend in NiMH HEV battery substitution by Li-ion continues, a recycling infrastructure built at the current level of EOL availability will be severely underutilized within a decade. The uncertainty about which future scenario plays out introduces a significant risk for large-scale investment. It can escalate the cost of capital and jeopardize the economic viability of domestic recycling as a source of critical materials. A potentially effective risk mitigation strategy would be to build smaller, distributed facilities, and invest in a larger network of warehouse storage facilities to maximize facility utilization. Moreover, as same storage facilities can serve other battery/battery material types, it could be repurposed if there is excess storage capacity. Storage creates greater flexibility and allows for high levels of processing facility utilization and overall lower costs irrespective of which scenario plays out.

Alternatively, designing recycling facilities to accommodate or flexibly adapt to other feedstock (e.g. Lithium-ion batteries, consumer electronics batteries) or even REE from primary sources could similarly mitigate risks as long as any technical challenges with mixed feed recycling can be resolved. For future analysis, one technology option for mitigating the uncertainty associated with the availability of EOL NiMH batteries in the U.S. is to establish an infrastructure capable of recycling both NiMH and LiBs. Liu et al. (Tian et al. 2019) describe such a process, and Rinne et al. (2021) present results from an LCA of the proposed process. Umicore has commercialized a process for recycling both lithium-ion and NiMH batteries. The first step in their process is a pyrometallurgical separation to produce an alloy of nickel, copper, and cobalt, which are then recovered as individual metals with hydrometallurgical methods. The individual rare earth contained in the slag produced during the pyrometallurgical processing of the NiMH batteries may be further separated, as described in this paper.

Whereas recycling logistics would more likely grow organically with multiple, independent stakeholders, the nationally optimized analysis described in this study enables a comprehensive techno-economic and life-cycle analysis of critical material recovery from EOL products and informs possible reverse battery supply chain strategies. For instance, the combination of locational marginal costs of battery processing and the relative contribution of battery acquisition costs can inform regionally targeted economic incentives or other policy mechanisms to improve battery collection such as requiring manufacturers to take ownership of EOL products or rewarding customers for delivering used batteries. A more targeted analysis in future could explicitly account for uncertainty and variations in EOL feedstock availability, regional regulatory constraints, and existing infrastructure, and build on the findings of this study to account for uncertain markets of recovered products, perform cash flow and conditional value at risk analysis, and address issues related to environmental and social justice.

STAR★METHODS

Detailed methods are provided in the online version of this paper and include the following:

- KEY RESOURCES TABLE
- RESOURCE AVAILABILITY

SUPPLEMENTAL INFORMATION

Supplemental information can be found online at https://doi.org/10.1016/j.isci.2022.104830.

ACKNOWLEDGMENTS

The submitted manuscript has been created by UChicago Argonne LLC, Operator of Argonne National Laboratory ("Argonne"). Argonne, a U.S. Department of Energy Office of Science laboratory, is operated under Contract No. DE-AC02-06CH11357. The U.S. Government retains for itself, and others acting on its behalf, a paid-up nonexclusive, irrevocable worldwide license in said article to reproduce, prepare derivative works, distribute copies to the public, and perform publicly and display publicly, by or on behalf of the Government. The Department of Energy will provide public access to these results of federally sponsored research in accordance with the DOE Public Access Plan. We would like to thank Alberta Carpenter (National Renewable Energy Laboratory) and Jeff Greenblatt (Emerging Futures LLC) for their critical review of this analysis.

AUTHOR CONTRIBUTIONS

C.O.I. conceived the study. C.O.I., A.S.X., D.J.G., and S.D.S. developed the analysis. A.S.X. and C.O.I. developed the optimization framework, with significant contributions from J.A. and K.S. All authors contributed to the analysis. C.O.I., A.S.X., D.J.G., and S.D.S. wrote the paper.

DECLARATION OF INTERESTS

The authors declare no competing interests.

Received: January 12, 2022
Revised: May 25, 2022
Accepted: July 20, 2022
Published: September 16, 2022

SUPPORTING CITATIONS

The following reference appears in the Supplemental information: Luiz Eduardo and Borges Mansur (2010), Murray and Glidewell (2019), Nassar and Fortier (2021), Peiró et al. (2013), Ruetschi et al. (1995), TBGFS, 2020, U.S. Census Bureau (2020).

REFERENCES

Agrawal, S., Singh, R.K., and Murtaza, Q. (2015). A literature review and perspectives in reverse logistics. Resour. Conserv. Recycl.

Ahn, N.-K., Shim, H.-W., Kim, D.-W., and Swain, B. (2020). Valorization of waste NiMH battery through recovery of critical rare earth metal: a simple recycling process for the circular economy. Waste Manag.

Akram, Abdul-Kader, W., and Abdul-Kader, W. (2021). Electric vehicle battery state changes and reverse logistics considerations. Int. J. Sustain. Eng. *14*, 390–403.

Al-Thyabat, S., Nakamura, T., Shibata, E., and Iizuka, A. (2013). Adaptation of minerals processing operations for lithium-ion (LiBs) and nickel metal hydride (NiMH) batteries recycling: critical review. Miner. Eng.

Arshi Praneet, S., Vahidi, E., and Zhao, F. (2018). Behind the scenes of clean energy: the environmental footprint of rare earth products. ACS Sustain. Chem. Eng. *6*, 3311–3320.

Assefi, M., Maroufi, S., Yamauchi, Y., and Sahajwalla, V. (2020). Pyrometallurgical recycling of Li-ion, Ni–Cd and Ni–MH batteries: a minireview. Current Opinion in Green and Sustainable Chemistry.

Azadnia, A.H., Onofrei, G., and Ghadimi, P. (2021). Electric vehicles lithium-ion batteries reverse logistics implementation barriers analysis: a TISM-MICMAC approach. Resour. Conserv. Recycl. *174*, 105751.

Bernard, P., and Lippert, M. (2015). Nickel–cadmium and nickel–metal hydride battery energy storage. Electrochemical Energy Storage for Renewable Sources and Grid Balancing,

223–51 (Elsevier). https://doi.org/10.1016/B978-0-444-62616-5.00014-0.

Biden, J.R. (2021). E.O. 14008 – Tackling the climate crisis at home and abroad. Vol. 86 FR 7619. https://www.federalregister.gov/documents/2021/02/01/2021-02177/tackling-the-climate-crisis-at-home-and-abroad.

Bösch, M.E., Hellweg, S., Huijbregts, M.A.J., and Frischknecht, R. (2006). Applying cumulative exergy demand (CExD) indicators to the ecoinvent database. Int. J. Life Cycle Assess. *12*, 181–190. https://doi.org/10.1065/lca2006.11.282o.

Bureau of Transportation Statistics (2020). Populated places. https://data-usdot.opendata.arcgis.com/datasets/populated-places.

Castilloux, R. (2016). Rare earth market outlook: supply, demand, and pricing from 2016 through 2025. In Market Report (Adamas Intelligence).

Castro, D. (2016). José, kelleher environmental, Gracestone Inc, and québec) commission for environmental cooperation (montréal. Environmentally Sound Management of End-of-Life Batteries from Electric-Drive Vehicles in North America. http://www.deslibris.ca/ID/10050890.

Ciez, R.E., and Whitacre, J.F. (2019). Examining different recycling processes for lithium-ion batteries. Nat. Sustain. *2*, 148–156. https://doi.org/10.1038/s41893-019-0222-5.

Ciroth, A., Di Noi, C., Lohse, T., and Srocka, M. (2020). OpenLCA 1.10 Comprehensive User Manual (GreenDelta, GmbH). https://www.openlca.org/wp-content/uploads/2020/02/openLCA_1.10_User-Manual.pdf.

Dai, Q., Spangenberger, J., Ahmed, S., Gaines, L., Kelly, J.C., and Wang, M. (2019). EverBatt: a closed-loop battery recycling cost and environmental impacts model. ANL *19/16*, 1530874. https://doi.org/10.2172/1530874.

Davis, S., and Gary Boundy, R. (2021). Transportation Energy Data Book: Edition 39. ORNL/TM-2020/1770. Oak Ridge National Lab. (ORNL), Oak Ridge, TN (United States). https://doi.org/10.2172/1767864.

Demirel, E., Demirel, N., and Gökçen, H. (2016). A mixed integer linear programming model to optimize reverse logistics activities of end-of-life vehicles in Turkey. J. Clean. Prod. *112*, 2101–2113.

Department of Defense. (2019). DOD Area Cost Factors (ACF) (Department of Defense). https://www.usace.army.mil/Cost-Engineering/Programming-Administration-and-Execution-System-Ne/.

DOE-EERE (2020). Department of Energy Issues Request for Information to Strengthen Battery Critical Materials Supply Chains (Energy.Gov). https://www.energy.gov/eere/articles/department-energy-issues-request-information-strengthen-battery-critical-materials.

Dunn, J.B., Gaines, L., Sullivan, J., and Wang, M.Q. (2012). Impact of recycling on cradle-to-gate energy consumption and greenhouse gas emissions of automotive lithium-ion batteries. Environ. Sci. Technol. *46*, 12704–12710. https://doi.org/10.1021/es302420z.

Ebin, B., Petranikova, M., and Ekberg, C. (2018). Physical separation, mechanical enrichment and recycling-oriented characterization of spent NiMH batteries. J. Mater. Cycles Waste Manag. *20*, 2027.

Ecoinvent Center (2018). Ecoinvent Database v3.5 (version 3.5). Zurich, Switzerland. https://www.ecoinvent.org/database/older-versions/ecoinvent-35/ecoinvent-35.html.

Ellis, T.W., and Mirza, A.H. (2014). Battery recycling: defining the market and identifying the technology required to keep high value materials in the economy and out of the waste dump. https://www.nist.gov/system/files/documents/2017/04/28/245_battery_recycling_defining_the_market.pdf.

European Commission Joint Research Centre (2012). Characterisation Factors of the ILCD-Recommended Life Cycle Impact Assessment Methods (European Union: Institute for Environment and Sustainability). EUR 25167EN-2012. https://eplca.jrc.ec.europa.eu/uploads/LCIA-characterization-factors-of-the-ILCD.pdf.

European Union (2020). Proposal for a Regulation of the European Parliament and of the Council Concerning Batteries and Waste Batteries, Repealing Directive 2006/66/EC and Amending Regulation (EU) No 2019/1020 (European Commission).

Fetcenko, M.A., Ovshinsky, S.R., Reichman, B., Young, K., Fierro, C., Koch, J., Zallen, A., Mays, W., and Ouchi, T. (2007). Recent advances in NiMH battery technology. J. Power Sources *165*, 544–551.

Frank, M. (2011). Cost Estimating Guide — DOE Directives, Guidance, and Delegations (Department of Energy). Directive DOE G 413.3-21. https://www.directives.doe.gov/.

Gaines, L. (2014). The future of automotive lithium-ion battery recycling: charting a sustainable course. Sustainable Materials and Technologies *1–2*, 2–7. https://doi.org/10.1016/j.susmat.2014.10.001.

Gohlke, D., and Zhou, Y. (2020). Assessment of Light-Duty Plug-In Electric Vehicles in the United States, 2010 – 2019 (Argonne National Lab. (ANL)). ANL/ESD-20/4. https://doi.org/10.2172/1642114.

Govindan, K., and Soleimani, H. (2017). A review of reverse logistics and closed-loop supply chains: a journal of cleaner production focus. J. Clean. Prod. *142*, 371–384.

Graedel, T.E., Harper, E.M., Nassar, N.T., Nuss, P., and Reck, B.K. (2015). Criticality of metals and metalloids. Proc. Natl. Acad. Sci. USA *112*, 4257–4262. https://doi.org/10.1073/pnas.1500415112.

He, M., Lin, T., Wu, X., Luo, J., and Peng, Y. (2020). A systematic literature review of reverse logistics of end-of-life vehicles: bibliometric analysis and research trend. Energies *13*, 5586.

Hendrickson, T.P., Kavvada, O., Shah, N., Sathre, R., and D Scown, C. (2015). Life-cycle implications and supply chain logistics of electric vehicle battery recycling in California. Environ. Res. Lett. *10*, 014011.

Holmberg, F. (2017). Recycling of Nickel Metal Hydride (NiMH) Batteries: Characterization and Recovery of Nickel, AB5 Alloy and Cobalt (Chalmers University). Thesis. http://publications.lib.chalmers.se/records/fulltext/249441/249441.pdf.

Huang, K., Jia, L., and Xu, Z. (2011). Enhancement of the recycling of waste Ni–Cd And Ni–Mh batteries by mechanical treatment. Waste Manage.

Idaho National Laboratory (2017). "Inl - DOE advanced vehicle testing activity." INL Advanced Vehicles. 2017. https://avt.inl.gov/.

Iloeje, C.O., Khalid, Y., Cresko, J., and Graziano, D.J. (2020). Assessing the techno-economic feasibility of solvent-based, critical material recovery from uncertain, end-of-life battery feedstock. In Energy Technology 2020: Recycling, Carbon Dioxide Management, and Other Technologies, First edition, X. Chen, Y. Zhong, L. Zhang, J.A. Howarter, A.A. Baba, C. Wang, and Z. Sun, et al., eds. (Springer International Publishing). The Minerals, Metals & Materials Series. https://doi.org/10.1007/978-3-030-36830-2.

Iloeje, C.O. (2019). SolventX - Solvent Extraction Model for Separating Rare Earth Mixtures (GitHub). https://github.com/solventx/solventx.

Iloeje, C.O., Jové Colón, C.F., Cresko, J., and Graziano, D.J. (2019). Gibbs energy minimization model for solvent extraction with application to rare-earths recovery. Environ. Sci. Technol. *53*, 7736–7745.

Innocenzi, V., Ippolito, N.M., De Michelis, I., Prisciandaro, M., Medici, F., and Vegliò, F. (2017). A review of the processes and lab-scale techniques for the treatment of spent rechargeable NiMH batteries. J. Power Sources *362*, 202–218.

Islam, M.T., and Huda, N. (2018). Reverse logistics and closed-loop supply chain of waste electrical and electronic equipment (WEEE)/E-Waste: a comprehensive literature review. Resour. Conserv. Recycl. *137*, 48–75.

Jha, Manis Kumar, Choubey, P., Dinkar, O., Panda, R., Jyothi, R., Yoo, K., and Park, I. (2022). Recovery of rare earth metals (REMs) from nickel metal hydride batteries of electric vehicles. Minerals *12*, 34.

Jin, H., Park, D.M., Gupta, M., Brewer, A.W., Ho, L., Singer, S.L., Bourcier, W.L., Woods, S., Reed, D.W., Lammers, L.N., et al. (2017). Techno-economic assessment for integrating biosorption into rare earth recovery process. ACS Sustain. Chem. Eng. *5*, 10148–10155. https://doi.org/10.1021/acssuschemeng.7b02147.

Kannan, G., Sasikumar, P., and Devika, K. (2010). A Genetic Algorithm Approach for Solving a Closed Loop Supply Chain Model: A Case of Battery Recycling (Applied Mathematical Modelling).

Kelleher Environmental, Gracestone, Inc., and Millette Environmental (2019). Research study on reuse and recycling of batteries employed in electric vehicles: The technical, environmental, economic, energy and cost implications of reusing and recycling ev batteries. https://www.api.org/~/media/Files/Oil-and-Natural-Gas/Fuels/Kelleher%20Final%20EV%20Battery%

20Reuse%20and%20Recycling%20Report%20to%20API%2018Sept2019%20edits%2018Dec2019.pdf.

Korkmaz, K., Alemrajabi, M., Rasmuson, Å.C., and Forsberg, K.M. (2020). Separation of valuable elements from NiMH battery leach liquor via antisolvent precipitation. Separ. Purif. Technol. *234*, 115812.

Lander, L., Cleaver, T., Rajaeifar, M.A., Nguyen-Tien, V., Elliott, R.J.R., Heidrich, O., Kendrick, E., Edge, J.S., and Offer, G. (2021). Financial viability of electric vehicle lithium-ion battery recycling. iScience *24*, 102787. https://doi.org/10.1016/j.isci.2021.102787.

Larsson, K., and Binnemans, K. (2014). Selective extraction of metals using ionic liquids for nickel metal hydride battery recycling. Green Chem. *16*, 4595–4603. https://doi.org/10.1039/C3GC41930D.

Liu, F., Peng, C., Porvali, A., Wang, Z., Wilson, B.P., and Lundström, M. (2019). Synergistic recovery of valuable metals from spent nickel–metal hydride batteries and lithium-ion batteries. ACS Sustain. Chem. Eng. *7*, 16103–16111.

Lombardo. (2020). USA rare earth acquires permanent magnet manufacturing capability. Charged EVs. https://chargedevs.com/newswire/usa-rare-earth-acquires-permanent-magnet-manufacturing-capability/.

Lu, S. (2006). Vehicle Survivability and Travel Mileage Schedules (U.S. Department of Transportation (NHTSA)). DOT HS 809 952. https://crashstats.nhtsa.dot.gov/Api/Public/ViewPublication/809952.

Marins, A.A.L., Banhos, S.G., Muri, E.J.B., Rodrigues, R.V., Cruz, P.C.M., and Freitas, M.B.J.G. (2020). Synthesis by coprecipitation with oxalic acid of rare earth and nickel oxides from the anode of spent Ni–mh batteries and its electrochemical properties. Mater. Chem. Phys. *242*, 122440.

Marins, A.A.L., Boasquevisque, L.M., Muri, E.J.B., and Freitas, M.B.J.G. (2022). Environmentally friendly recycling of spent Ni–MH battery anodes and electrochemical characterization of nickel and rare earth oxides obtained by sol–gel synthesis. Mater. Chem. Phys. *280*, 125821.

Maroufi, S., Khayyam Nekouei, R., Hossain, R., Assefi, M., and Sahajwalla, V. (2018). Recovery of Rare Earth (Ie, La, Ce, Nd, and Pr) Oxides from End-Of-Life Ni-MH Battery via Thermal Isolation (ACS Sustainable Chemistry & Engineering).

McKinley, C., and Ghahreman, A. (2018). Hydrochloric acid regeneration in hydrometallurgical processes: a review. Miner. Process. Extr. Metall. (IMM Trans. Sect. C) *127*, 157–168.

McRae, E.M. (2021). Nickel Statistics and Information (U.S. Geological Survey). https://www.usgs.gov/centers/nmic/nickel-statistics-and-information.

Melin, H.E., Rajaeifar, M.A., Ku, A.Y., Kendall, A., Harper, G., and Heidrich, O. (2021). Global implications of the EU battery regulation. Science *373*, 384–387.

Mohr, M., Peters, J.F., Baumann, M., and Weil, M. (2020). Toward a cell-chemistry specific life cycle assessment of lithium-ion battery recycling processes. J. Ind. Ecol. *24*, 1310–1322. https://doi.org/10.1111/jiec.13021.

Motorcells Hybrid Battery Renewal & Installation (2018). The ultimate guide to toyota prius battery problems. Hybrid Battery Repair Service (blog). https://hybridbatteryrepairservice.com/prius/.

Murray, D., and Glidewell, S. (2019). An Analysis of the Operational Costs of Trucking: 2019 Update (American Transportation Research Institute). https://truckingresearch.org/wp-content/uploads/2019/11/ATRI-Operational-Costs-of-Trucking-2019-1.pdf.

Nassar, N.T., and Fortier, S.M. (2021). Methodology and technical input for the 2021 review and revision of the U.S. Critical minerals list." USGS numbered series 2021–1045. Methodology and Technical Input for the 2021 Review and Revision of the U.S. Critical Minerals List. Open-File Report*2021–1045* (U.S. Geological Survey). https://doi.org/10.3133/ofr20211045.

Ni, Z., Chan, H.K., and Tan, Z. (2021). Systematic literature review of reverse logistics for E-waste: overview, analysis, and future research agenda. Int. J. Logist. Res. Appl. 1–29.

O'Dell, J. (2014). What happens to EV and hybrid batteries?" *Edmunds* (blog). https://www.edmunds.com/fuel-economy/what-happens-to-ev-and-hybrid-batteries.html.

Peters, M., Timmerhaus, K., and West, R. (2002). Plant Design and Economics for Chemical Engineers, 5th ed (McGraw-Hill Education).

Pinheiro, R.F., Michielin, L., Martins, T.R., Wildgrube, T., Tanabe, E.H., and Bertuol, D.A. (2021). Application of mechanical processing operations for the recycling of nickel metal hydride batteries. J. Mater. Cycles Waste Manag. *23*, 2148–2161.

Poulton, M.M., Jagers, S.C., Linde, S., Van Zyl, D., Danielson, L.J., and Matti, S. (2013). State of the world's nonfuel mineral resources: supply, demand, and socio-institutional fundamentals. Annu. Rev. Environ. Resour. *38*, 345–371. https://doi.org/10.1146/annurev-environ-022310-094734.

Qiao, Q., Zhao, F., Liu, Z., and Hao, H. (2019). Electric vehicle recycling in China: economic and environmental benefits. Resour. Conserv. Recycl. *140*, 45–53. https://doi.org/10.1016/j.resconrec.2018.09.003.

Rajaeifar, Ghadimi, P., Raugei, M., Wu, Y., Heidrich, O., and Heidrich, O. (2022). Challenges and recent developments in supply and value chains of electric vehicle batteries: a sustainability perspective. Resour. Conserv. Recycl. *180*, 106144.

Rasoulnia, P., Barthen, R., Puhakka, J.A., and Lakaniemi, A.-M. (2021). Leaching of rare earth elements and base metals from spent NiMH batteries using gluconate and its potential bio-oxidation products. J. Hazard Mater. *414*, 125564.

Riddle, M.E., Tatara, E., Olson, C., Smith, B.J., Bennett Irion, A., Harker, B., Pineault, D., Alonso, E., and Graziano, D.J. (2021). Agent-based modeling of supply disruptions in the global rare earths market. Resour. Conserv. Recycl. *164*, 105193.

Rinne, M., Elomaa, H., Porvali, A., and Lundström, M. (2021). Simulation-based life cycle assessment for hydrometallurgical recycling of mixed LIB and NiMH waste. Resour. Conserv. Recycl. *170*, 105586.

Luiz Eduardo, O.C.R., and Borges Mansur, M. (2010). Hydrometallurgical separation of rare earth elements, cobalt and nickel from spent nickel–metal–hydride batteries. J. Power Sources *195*, 3735–3741. https://doi.org/10.1016/j.jpowsour.2009.12.071.

Ruetschi, P., Meli, F., Desilvestro, J., Felix, M., and johann, D. (1995). nickel-metal hydride batteries the preferred batteries of the future? J. Power Sources *57*, 85–91. https://doi.org/10.1016/0378-7753(95)02248-1.

Sabatini, J.C., Field, E.L., Wu, I.C., Cox, M.R., Barnett, B.M., and Coleman, J.T. (1994a). Feasibility study for the recycling of nickel metal hydride electric vehicle batteries. NREL. Report NREL/TP-463-6153.

Sabatini, J.C., Field, E.L., Wu, I.C., Cox, M.R., Barnett, B.M., and Coleman, J.T. (1994b). Feasibility study for the recycling of nickel metal hydride electric vehicle batteries (National Renewable Energy Lab.; Little (Arthur D.), Inc.). Final Report." NREL/TP-4636153. https://doi.org/10.2172/10129037.

Salim, H.K., Stewart, R.A., Sahin, O., and Dudley, M. (2019). Drivers, barriers and enablers to end-of-life management of solar photovoltaic and battery energy storage systems: a systematic literature review. J. Clean. Prod. *211*, 537–554.

Silvestri, L., Forcina, A., Arcese, G., and Bella, G. (2020). Recycling technologies of nickel–metal hydride batteries: an LCA based analysis. J. Clean. Prod. *273*, 123083.

Supekar, S.D., and Skerlos, S.J. (2017). Analysis of costs and time frame for reducing CO_2 emissions by 70% in the U.S. Auto and energy sectors by 2050. Environ. Sci. Technol. *51*, 10932–10942.

Tadaros, M., Migdalas, A., Samuelsson, B., and Segerstedt, A. (2020). Location of facilities and network design for reverse logistics of lithium-ion batteries in Sweden. Oper. Res. Int. J. *22*, 895–915.

Peiró, Talens, Villalba Méndez, G., and Villalba Méndez, G. (2013). Material and energy requirement for rare earth production. JOM *65*, 1327–1340. https://doi.org/10.1007/s11837-013-0719-8.

Tatarevic, B. (2016). Original hybrid batteries still charged up 15 Years later. The Truth About Cars (blog). https://www.thetruthaboutcars.com/2016/07/original-hybrid-batteries-still-charged-15-years-later/.

Taylor, B. (2019). A detour for nickel. Recycling today. https://www.recyclingtoday.com/article/nickel-scrap-commodity-focus-june-2019/.

TBGFS (2020). Trans-Border Global Freight Systems, Inc. - Freight Logistics - TBGFS (Official. Trans-Border Global Freight Systems, Inc). https://www.tbgfs.com/.

Thompson, D., Hyde, C., Hartley, J.M., Abbott, A.P., Anderson, P.A., and Harper, G.D.J. (2021). To shred or not to shred: a comparative techno-economic assessment of lithium ion battery hydrometallurgical recycling retaining value and improving circularity in LIB supply chains. Resour. Conserv. Recycl. *175*, 105741. https://doi.org/10.1016/j.resconrec.2021.105741.

Tian, Y., Liu, Z., and Zhang, G. (2019). Recovering REEs from NdFeB wastes with high purity and efficiency by leaching and selective precipitation process with modified agents. J. Rare Earths *37*, 205–210. https://doi.org/10.1016/j.jre.2018.10.002.

Tuck, C.A. (2020). Iron and Steel Scrap Data Sheet - Mineral Commodity Summaries (U.S. Geological Survey). https://www.usgs.gov/centers/nmic/iron-and-steel-scrap-statistics-and-information.

U.S. Census Bureau (2020) (The U.S. Census Bureau." U.S. Department of Commerce). https://www.commerce.gov/bureaus-and-offices/census.

U.S. Department of Energy (2021). Critical Minerals and Materials: U.S. Department of Energy's Strategy to Support Domestic Critical Mineral and Material Supply Chains (FY 2021-FY 2031). https://www.energy.gov/sites/prod/files/2021/01/f82/DOE%20Critical%20Minerals%20and%20Materials%20Strategy_0.pdf.

U.S. Department of Transportation Federal Highway Administration (2019). Average Age of Automobiles and Trucks in Operation in the United States." National Transportation Statistics. Table 1-26). https://rosap.ntl.bts.gov/gsearch?collection=dot:35533&type1=mods.title&fedora_terms1=National+Transportation+Statistics.

U.S. Environmental Protection Agency (2020). EGRID2018 Summary Data. https://www.epa.gov/sites/default/files/2020-01/egrid2018_summary_tables.xlsx.

U.S. Geological Survey (2020a). Mineral Commodity Summaries 2020. https://pubs.usgs.gov/periodicals/mcs2020/mcs2020.pdf.

U.S. Geological Survey (2020b). Mineral Commodity Summaries 2020." Technical Report (U.S. Geological Survey). https://doi.org/10.3133/mcs2020.

United States Census Bureau (2020). TIGER/Line Shapefiles (The United States Census Bureau). https://www.census.gov/geographies/mapping-files/time-series/geo/tiger-line-file.html.

US Bureau of Labor Statistics (2020). Producer price indices. http://www.bls.gov/ppi/.

Wang, L., Wang, X., and Yang, W. (2020a). Optimal design of electric vehicle battery recycling network–from the perspective of electric vehicle manufacturers. Appl. Energy *275*, 115328.

Wang, M., Elgowainy, A., Lu, Z., Bafana, A., Benavides, P., Burnham, A., Cai, H., et al. (2020b). Greenhouse Gases, Regulated Emissions, and Energy Use in Technologies Model ® (2020 .Net) (Argonne National Laboratory (ANL)). (United States). https://doi.org/10.11578/GREET-NET-2020/DC.20200913.1.

Wang, S., Yu, J., and Okubo, K. (2021). Life cycle assessment on the reuse and recycling of the nickel-metal hydride battery: fleet-based study on hybrid vehicle batteries from Japan. J. Ind. Ecol. *25*, 1236–1249. https://doi.org/10.1111/jiec.13126.

Watari, T., Nansai, K., Giurco, D., Nakajima, K., McLellan, B., and Helbig, C. (2020). Global metal use targets in line with climate goals. Environ. Sci. Technol. *54*, 12476–12483.

Williams, R., Jr. (1947). Six-Tenths Factor Aids in Approximating Costs (Chemical Engineering Magazine).

Xavier, A.S., Chukwunwike, O., and Iloeje. (2020). RELOG: Reverse Logistics Optimization (Argonne National Laboratory). https://anl-ceeesa.github.io/RELOG/0.5/.

Xu, P., Dai, Q., Gao, H., Liu, H., Zhang, M., Li, M., Chen, Y., An, K., Meng, Y.S., Liu, P., et al. (2020). Efficient direct recycling of lithium-ion battery cathodes by targeted healing. Joule *4*, 2609–2626. https://doi.org/10.1016/j.joule.2020.10.008.

Yang, X., Zhang, J., and Fang, X. (2014). Rare earth element recycling from waste nickel-metal hydride batteries. J. Hazard Mater. *279*, 384–388.

Young, K., Wang, C., Wang, L.Y., and Strunz, K. (2013). Electric vehicle battery technologies. In Electric Vehicle Integration into Modern Power Networks, *15–56*, R. Garcia-Valle and J.A. Peças Lopes, eds (Springer New York). https://doi.org/10.1007/978-1-4614-0134-6_2.

Yu, Y., Chen, B., Huang, K., Wang, X., and Wang, D. (2014). Environmental impact assessment and end-of-life treatment policy analysis for Li-ion batteries and Ni-MH batteries. Int. J. Environ. Res. Public Health *11*, 3185–3198. https://doi.org/10.3390/ijerph110303185.

Zhang, X., Li, L., Fan, E., Xue, Q., Bian, Y., Wu, F., and Chen, R. (2018). Toward sustainable and systematic recycling of spent rechargeable batteries. Chem. Soc. Rev. *47*, 7239–7302.

Zhi, H., Ni, S., Su, X., Xie, W., Zhang, H., and Sun, X. (2021). Separation and recovery of rare earth from waste nickel-metal hydride batteries by phosphate based extraction-precipitation. J. Rare Earths *40*, 974–980.

STAR★METHODS

KEY RESOURCES TABLE

REAGENT or RESOURCE	SOURCE	IDENTIFIER
Deposited data		
Input and Output data for this study	This paper	ZENODO: https://doi.org/10.5281/zenodo.6812328
Software and algorithms		
RELOG	Argonne National Laboratory https://anl-ceeesa.github.io/RELOG	ZENODO: https://doi.org/10.5281/zenodo.5131239

RESOURCE AVAILABILITY

Lead contact

Further information and requests for resources and reagents should be directed to and will be fulfilled by the lead contact, Chukwunwike Iloeje (ciloeje@anl.gov)

Materials availability

This study did not generate new materials

Data and code availability

- Data: Input files used to generate both scenarios (in JSON format) as well as the results data (in CSV format) have been deposited at Zenodo (https://doi.org/10.5281/zenodo.6812328) and are publicly available as of the date of publication.
- Code: The source code for the reverse logistics optimization model has been deposited at Zenodo (https://doi.org/10.5281/zenodo.5131239) and is publicly available as of the date of publication.
- Any additional information required to reanalyze the data reported in this paper is available from the lead contact upon request.

METHOD DETAILS

We estimate the cost, energy, material flows and GHG impacts associated with recycling spent NiMH batteries using an approach that accounts for stocks, time-resolved availability and the logistics of procuring spent NiMH batteries from battery collection to the final recovered materials. The analysis framework adopted comprises five main components: recycling process techno-economics, spent battery scrappage and distribution, materials wedge analysis, reverse logistics optimization, and environmental impact assessment.

Recycling process techno-economics

In general, NiMH battery recycling involves a combination of mechanical/physical and chemical separations to recover target materials, traditionally via hydrometallurgical or pyro-metallurgical routes (Larsson and Binnemans 2014; Yang et al. 2014; Holmberg 2017; Zhang et al., 2018; Maroufi et al., 2018; Ahn et al., 2020; Assefi et al., 2020; Ellis and Mirza 2014; Huang et al. 2011; Al-Thyabat et al., 2013; Ebin et al. 2018). In this study, we focus on hydrometallurgical recovery. Figure S1 shows key components of the recycling unit processes — disassembly, cathode material recovery, anode material recovery and REE separations. The material balance model for the disassembly, cathode and anode processing units is based on the "physical separation/chemical process" configuration described by Sabatini et al., (1994a), where each dotted box shown in Figure S1 represents a conceptual grouping of operations that may take place in multiple equipment. The disassembly unit accepts the NiMH battery and delivers cathode, anode, casing and scrap material streams, as well as the electrolyte drain, which is reused downstream in a co-located cathode material recovery plant. The cathode processing unit recovers pure nickel, scrap metal, and some metallic hydroxide residues. The anode processing unit recovers more scrap metal, hydroxide residues and a REE chloride mixture. Each of the above units also include equipment and infrastructure for waste treatment. Table S8 shows the energy intensity of these subprocesses and the mass ratios of feeds crossing between them.

Table S9 shows the battery composition adopted in this study, which was derived from a number of literature sources. These sources generally reported different compositions, which reflect technology variation and evolution (e.g., change from metallic to mostly plastic casing). We also estimated an average battery weight of 46 kg by combining battery specification data from various sources for different, battery models (Davis and Gary Boundy, 2021; Castro, 2016; Kelleher Environmental, Gracestone, Inc., and Millette Environmental 2019; Young et al., 2013; Idaho National Laboratory 2017).

The REE separations facility includes the solvent extraction column, and several post-extraction equipment. The solvent extraction column receives the REE mixture and separates them into individual REEs or clusters, depending on separation target. We make the simplifying assumption that the rare earth mixture from the upstream cathode material recovery unit is free of contaminants. The presence of contaminants will require additional processing to separate, but the additional cost should be small compared to the overall cost of the integrated facility, and within the 30%–40% margin of error assumed for this class of preliminary cost estimates (Frank 2011). For this study, we consider separation into Nd-Pr (neodymium-praseodymium or didymium) and Ce-La (cerium-lanthanum) clusters. The electrowinning units convert the recovered REE chlorides from the solvent extraction process into higher-value REE alloys. The solvent extraction process model used in this study is described in earlier work (Chukwunwike O. Iloeje et al., 2019), with an open-source implementation available on Github (C. O Iloeje 2019).

The economic analysis applies a bottoms-up approach that uses the sizing information from the process models to evaluate corresponding equipment costs (C_{equip}), capital costs (C_{capex}) and operating costs (C_{opex}) for each facility. The overall economic model follows the approach described in Peters & Timmerhaus (Peters et al. 2002) for capital engineering projects. Equations 1–3 summarize the economic formulation for the plant costs. For each facility unit,

$$C_{equip} = \sum_i \left(C_{ref_i} (\beta)^n * N_i * \Psi_{PPI}\right) \quad \text{(Equation 1)}$$

$$C_{capex} = C_{equip}\left(1 + f_{delivery}\right)\left(1 + \sum f_d + \sum f_{ind}\right) \quad \text{(Equation 2)}$$

$$C_{opex} = \sum_k f_k C_k + \sum_j m_j C_j \quad \text{(Equation 3)}$$

Here, C_{ref_i} is the reference cost of the corresponding equipment i ; $(\beta)^n$ is the scaling parameter (Peters et al. 2002; Williams, 1947) based on the ratio of actual to reference facility feed mass flow rates; N_i represents the number of units of equipment i; and the Ψ_{PPI} term uses the producer price index (US Bureau of Labor Statistics 2020) to convert equipment prices from the reference year to the project's currency year equivalent. The capital cost is determined by multiplying the total equipment cost with factors that capture contributions from direct costs (f_d) like equipment delivery and installations, and from indirect costs (f_{ind}) like supervision and contingency. Operating costs include the summed contributions from variable and fixed costs. For the variable cost component, m_j represents the relevant quantity (e.g., solvents, process water) and C_j represents the cost per unit quantity. For the fixed costs, f_k represents the multiplier factor for each cost item (e.g., taxes), and C_k is their associated cost basis (e.g., fixed capital). Tables S2–S7 summarize the relevant parameter values and cost factors used in determining the operating cost items.

Analysis scenarios

In this study, we consider two possible future scenarios for HEV sales projections to provide lower and upper bound estimates for the quantity of spent NiMH batteries available for recycling. A "conservative" scenario projects a decline in the proportion of NiMH batteries in HEVs owing to substitution by LiBs as demonstrated by recent historical trends. To create this projection, we use historic HEV sales data (Gohlke and Zhou 2020) to determine the trend in NiMH proportion of HEV batteries, then use a sigmoid function extrapolate the historical trend out in to the future. The sigmoid function extrapolates a 3-year moving average fit of the historical data to avoid bias from recorded data fluctuations. The "optimistic" scenario assumes that the proportion of NiMH batteries in HEVs will stay constant in future years. To create this scenario projection, we fix the NiMH proportion of HEV batteries at the 2019 level, and assume this proportion is maintained going forward into the future. This represents an optimistic outlook where other factors such as economics, improvements in NiMH technology, or changes in demand keep NiMH batteries relatively competitive. While less likely, this scenario still represents a useful upper-bound for our analysis.

End-of-life battery scrappage, source distribution and collection

Vehicle scrappage probability density function (PDF), denoted by *f(t)*, where *t* is the age of the vehicle, is assumed to follow a logistic distribution based on similar formulations in the literature . As described earlier, we assume that the scrappage rate of batteries is equivalent to that of vehicles. The scrappage PDF takes the form shown in Equation 4, wherein μ is the median lifespan of the vehicle in years and *s* is a shape parameter proportional to the standard deviation of vehicle lifespans in years.

$$f(t) = \frac{e^{\frac{t-\mu}{s}}}{\sigma\left(1+e^{\frac{t-\mu}{s}}\right)^2} \quad \text{(Equation 4)}$$

The cumulative scrappage probability, *F(t)*, where *t* is the age of the vehicle, is therefore the integral of *f(t)* as shown in Equation 5.

$$F(t) = \int_{-\infty}^{t} \frac{e^{\frac{x-\mu}{s}}}{\sigma\left(1+e^{\frac{x-\mu}{s}}\right)^2} dx = \frac{1}{1+e^{-\left(\frac{t-\mu}{s}\right)}} \quad \text{(Equation 5)}$$

Both μ and *s* are assumed to remain constant across HEV model years in this study. The value of μ is set to 12 years following data from the U.S. Dept. of Transportation(U.S. Department of Transportation Federal Highway Administration 2019). The shape parameter *s* is set to 2 years to allow for a larger spread in the distribution following vehicle survivability data from the U.S. Dept. of Transportation (Lu 2006). Substituting these values μ and *s* in Equation 5, the cumulative scrappage probability is expressed in Equation 6. The PDF and its corresponding cumulative distribution function are shown in Figure S3.

$$F(t) = \frac{1}{1+e^{-\left(\frac{t-12}{2}\right)}} \quad \text{(Equation 6)}$$

Let $S(k)$ denote the number of vehicles sold at year k. The number of vehicles scrapped at year k, denoted by $d(k)$, was calculated as shown in Equation 7, where j is the index for vehicle age and $F(j)$ is given by Equation 6. The index k refers to a specific year within the analysis time horizon of Y years, and thus $k \in [1, 2, .., Y]$. We also define the practical lifespan of a vehicle, T, for which $F(T) \approx 1$. For the values of μ and s chosen in this study, $T = 32$ years captures 99.995% of all vehicles scrappage and is therefore a conservative choice as a practical lifespan for all vehicles.

$$d(k) = \left\{ \begin{array}{ll} S(k)F(j) & : k = 1 \\ \sum_{j=1}^{\min(k,T)} S(k-j+1)F(j) - \sum_{j=1}^{\min(k-1,T-1)} S(k-j)F(j) & : k > 1 \end{array} \right\} \quad \text{(Equation 7)}$$

It should be noted that $d(k)$ is not cumulative; that is, it represents scrappage of vehicles that have been scrapped between year k and its previous year; it does not represent the totality of vehicles scrapped until year k. Further, $d(k)$ accounts for all vehicles of all ages between 0 and T in year k following from the scrappage probability function. To estimate the quantities and distribution of spent NiMH batteries across the continental U.S. at county resolution, we first multiply the annual scrappage projection from the stock flow model with the normalized HEV sales data (equivalent HEV market share by state) to determine state-level quantities. Then, within each state, we use the major city/populated places data to approximate quantities of spent batteries at the city level. Here we define a major city as one with a minimum population threshold of 10,000. County-level data is obtained by summing annual battery stocks from all the cities associated with the county. Figure S4A shows the resulting spent NiMH battery distribution heat map, with counties in California having the highest spent batteries densities. Figure S4B shows the top 10 continental U.S. states which account for 75% of the spent batteries, with California accounting for just over 45%.

To build out the reverse logistics pipeline, we assume that these spent batteries are stocked in collection centers distributed across different counties in the U.S. Assuming that a majority of HEV vehicles are located in urban areas, collection centers are considered only in cities with populations greater than the specified threshold. These collection centers may represent vehicle graveyards or mechanic shops/dealerships that collect spent HEV batteries when individual consumers get their battery replaced or dispose of their used vehicles. For the reference case, we assume that only a fraction ($\beta = 50\%$) of the spent batteries are available for recycling, and estimate the amount of batteries arriving at each collection center using Equation 8, where $N_{batt,i}$ is the number of batteries at each collection center i, $N_{tot\ batt}$ is the total number of available spent batteries, S_{state} is the corresponding state-level HEV market share, Pop_i is the population

of the given collection center's city and $StatePop_{city}$ is the total population of all cities in the state. Figure S4C, shows the resulting distribution of the collection centers, where the marker shade reflects the relative number of batteries at the collection center.

$$N_{batt,i} = \beta * N_{totbatt} * S_{state} * \frac{Pop_i}{StatePop_{city}} \quad \text{(Equation 8)}$$

Some relevant data sources for this analysis include geographic information system (GIS) data for the U.S. highway network, 2010 census data for each city and state in the U.S., statewide HEV sales data to determine the proportional distribution of batteries by state, and location-based capital project cost factors based on U.S. Department of Defense numbers for normalizing project costs across states (Department of Defense 2019; Bureau of Transportation Statistics 2020; United State Census Bureau, 2020; United States Census Bureau 2020). These regional cost factors multiply capital cost to reflect the differences in project costs across states. The transportation routes between collection centers and plants are straight-line approximations; while this underestimates the total transport distance, randomly sampled comparisons show that they rarely deviate more than 5–7% from values obtained from detailed road network tracing.

Wedge analysis

The wedge analysis focuses on didymium and nickel metal saleable products from the recycling complex, for which the U.S. currently has no production capacity. We assess the extent to which the NiMH recycling complex could provide a domestic source of these metals that are critical for cleaner energy technologies by comparing the "wedge" of annual secondary supply streams of materials from NiMH recycling to the "wedge" of annual demand of those materials in a certain context. Table S16 provides a comparison of the maximum recovery of these materials from NiMH recycling with estimates of their U.S. production and demand.

The primary applications for didymium are for the manufacture of NdFeB magnets and other alloys. The U.S. currently has manufacturing capacity for bonded but not for sintered NdFeB magnets used in cleaner energy technologies. Current U.S. demand for didymium was estimated from information in the Adamas Report (Castilloux 2016). A step-up in U.S. demand is expected, however, from USA RareEarth LLC's purchase of sintered NdFeB magnet manufacturing equipment that was formerly owned and operated by Hitachi Metals America, Ltd in North Carolina. With a reported capacity of 2000 tpy NdFeB and assuming a 30% didymium content, demand for the didymium alloy for such a plant would be on the order of 600 tpy.

Applications for Ni metal include stainless steel, other steel alloys, superalloys, electroplating, catalysts, and chemicals (U.S. Geological Survey 2020b). Demand for nickel is expected to significantly increase as global production of LiBs for electric vehicles steadily expands (Taylor 2019). Because the U.S. demand for the recovered products is significantly higher than the tonnages recoverable from the NiMH recycling complex, we instead compare the annual recovered tonnages to the tonnages of Nd/Pr and Ni metals in the U.S. sales of HEVs containing NiMH batteries.

Reverse logistics optimization

Our implementation of the resulting mixed-integer linear reverse logistics problem has been made publicly available as RELOG (Xavier et al., 2020), an open-source software package for reverse logistics optimization. The package could also be used more broadly in modeling and analysis of customized reverse logistics pipelines with multiple types of plants, multiple types of products, multiple time periods, and allows for storage and plant capacity expansion. The modeling assumptions and a simplified mathematical formulation of the problem are described briefly here.

In RELOG, reverse logistics pipelines are described by two main model components: (1) *products and materials*; and (2) *processing plants*. In this analysis, we had 14 types of products and materials: (1) NiMH batteries; (2) cathode; (3) anode; (4) nickel (Ni) metal; (5) nickel-iron (Ni-Fe) scrap; (6) iron-nickel (Fe-Ni) scrap; (7) mixed hydroxides; (8) mixed REE chlorides (Rare-Earth Mix); (9) didymium (Nd-Pr) alloy; (10) cerium-lanthanum (Ce-La) alloy; (11) mischmetal (misch) alloy; (12) leach residue; (13) salt; and (14) plastic pack. NiMH batteries are the primary source materials. Cathode, anode and mixed REE chlorides are intermediate products, whereas the remaining products are final products. We have four types of processing plants: (1) disassembly plants, (2) anode material recycling plants, (3) cathode material recycling plants, and (4) rare-earth separation plants. In RELOG, plants receive a single type of material and convert it into multiple

others. Figure S5 illustrates the inputs and outputs for each type of plant in this case study. For example, disassembly plants receive NiMH batteries as input and produce anode, cathode, iron-nickel scrap and plastic packs. In this study, we enforced colocation for the different types of plants.

RELOG assumes that source materials (spent NiMH batteries in this case study) are initially available at specific locations known as collection centers, which are described by their latitude, longitude and the amount of material available per year, in tonnes. All other products only become available during the recycling process. Transporting products from one location to another incurs a transportation cost ($/km/tonne). To process each tonne of material, the model assumes that plants incur a variable operating cost ($/tonne). Plants also incur a fixed operating cost ($) per year regardless of the amount of material they process, as long as they are open. Plants can be built at specified candidate locations (See Figure S6). Opening a plant incurs a one-time opening cost ($), which is region-specific. Plants also have a limited capacity (in tonnes), which indicates the maximum amount of input material they are able to process per year (set at $\leq 6,000$ tonnes of battery per year for this study). For each candidate location, we also specify minimum and maximum capacity of the plants that can be built at that particular location. Different plants sizes have different opening costs and fixed operating costs. After a plant is built, it can be further expanded in the following years, up to its maximum capacity. Products received by a plant can be either processed immediately or stored for later processing. Plants have a maximum storage capacity (tonne), and there are storage costs ($/tonne). All products generated by a plant can either be sent to another plant for further processing or disposed of locally for a cost ($/tonne).

The mathematical formulation of the resulting mixed-integer linear optimization problem solved by RELOG a variation of the *facility location* problem, a classical and widely studied problem in Operations Research. Our specific variation is a multi-echelon, multi-period facility location problem, with storage and plant expansion. To simplify the exposition, we assume that we have a single type of plant. We refer to RELOG's documentation (Xavier et al., 2020) for a more complete description. Let L be the set of collection centers holding the NiMH batteries to be recycled, let M be the set of final products recovered during the recycling process, let P be the set of potential plants to open, and let $T = \{1, \ldots, t^{max}\}$ be the set of years in the planning horizon. In summary, we must decide (i) where and when to open facilities; (ii) how much capacity should facilities have, and should they be expanded; (iii) how much material should be processed or stored during each year; and (iv) how should the material flow across the network. We minimize the overall fixed, variable, transportation and storage costs:

$$\begin{aligned} minimize \sum_{t\in T}\sum_{p\in P}\left[f_{tp}^{open}\left(u_{pt}\right) + f_{tp}^{fixed}\left(x_{pt}\right)\right] + \sum_{t\in T}\sum_{p\in P}\left[f_{tp}^{store}\left(z_{pt}^{store}\right) + f_{tp}^{proc}\left(z_{pt}^{proc}\right)\right] \\ + \sum_{t\in T}\sum_{p\in P} f_{tp}^{expand}\left(w_{p1}, \ldots, w_{pt}\right) + \sum_{t\in T}\sum_{l\in L}\sum_{p\in P} f_{tlp}^{tr}\left(y_{lpt}\right) \end{aligned} \quad \text{(Equation 9)}$$

Where f_{tp}^{open}, f_{tp}^{fixed}, f_{tp}^{expand}, f_{tp}^{store} and f_{tp}^{proc} are linear functions computing, respectively: the cost of opening p at year t; the fixed cost of keeping plant p operational; the cost of expanding plant p, as well as the increase in fixed operating costs generated by all previous expansions; the cost of storing material; and the cost of processing material. The linear function f_{tlp}^{tr} computes the cost of transporting material from collection center l to plant p. The constraints are as follows.

All batteries must be sent to a plant:

$$\sum_{p\in P} y_{lpt} = m_{lt}^{initial} \;\forall l \in L, t \in T \quad \text{(Equation 10)}$$

Amount received equals amount processed plus stored:

$$\sum_{l\in L} y_{lpt} + z_{p,t-1}^{store} = z_{pt}^{proc} + z_{p,t}^{store} \;\forall p \in P, t \in T \quad \text{(Equation 11)}$$

Plants have a limited processing capacity. Furthermore, if a plant is closed, it has zero processing capacity:

$$z_{pt}^{proc} \leq m_{p}^{min} x_p + \sum_{i=1}^{t} w_p \;\forall p \in P, t \in T \quad \text{(Equation 12)}$$

Plants have limited storage capacity. Furthermore, all material must be processed by the end of the planning horizon:

$$z^{store}_{pt,0} \leq m^{store}_{p} x_p \ \forall p \in P, t \in T$$
$$z^{store}_{p,t^{max}} = 0 \ \forall p \in P \quad \text{(Equation 13)}$$

Plants can only be expanded up to their maximum capacity. Furthermore, if a plant is closed, it cannot be expanded:

$$\sum_{i=1}^{t} w_p \leq m^{max}_{p} x_p \ \forall p \in P, t \in T \quad \text{(Equation 14)}$$

A plant is operational at year t if it was operational at time $t-1$ or it was built at year t. This constraint also prevents a plant from being built multiple times.

$$x_{pt} = x_{p,t-1} + u_{pt} \ \forall p \in P, t \in T \quad \text{(Equation 15)}$$

In the constraints above, $m^{initial}_{lp}$, m^{min}_{p}, m^{store}_{p} and m^{max}_{p} are constants representing, respectively: the amount of NiMH batteries available at collection center l at year t; the minimum capacity of plant p, if the plant is opened; the storage capacity of plant p; and the maximum processing capacity of plant p. The binary variables u_{pt} and x_{pt}, indicate that plant p starts operating, or stays operational in year t respectively; w_{pt} describes the extra capacity (amount above the minimum) added to plant p during year t; y_{lpt} describes the amount of material sent from collection center l to plant p during year t; z^{store}_{pt} represents the amount of material in storage at plant p at the end of year t, and z^{proc}_{pt} represents the amount of material or processed by plant p during year t. All decision variables are non-negative.

In the full optimization model, we have additional decision variables to keep track of the amount of product produced by each plant, as well as the amounts disposed. Products and materials recovered by one plant may be sent to another for further processing. Note that energy expenditure and emissions are not decision variables; these values are computed after an optimal solution is found, based on the values of the x, y, and z variables. For this case study, we defined a simulation window from 2025 to 2050, and assume that no plants are closed during period. We allow for annual feedstock storage of up to 3 months of maximum capacity at each facility, at the reference value of $150/tonne/year.

Life cycle assessment

Environmental impacts of the battery collection and recycling process are calculated using life cycle assessment (LCA) in accordance with ISO14040/44 guidelines. The functional unit used for this attributional LCA analysis is 1000 kg of NiMH battery scrap input (composition shown in Table S9) to the recycling facility. Processes within the scope of the LCA include those associated with the transportation of spent batteries from a central collection facility to the recycling facility, energy and material inputs to the battery recycling process (includes upstream impacts), and any air emissions, water emissions, and waste treatment processes resulting from the recycling process. Transportation impacts from battery end-users to the central battery collection facility as well as impacts from transporting useful recycling products to their next life cycle are excluded. Embodied energy and emissions in the spent battery itself from its previous slife cycle are also excluded from the analysis. In the interest of transparency, the analysis does not assume displacement of primary production of economically valuable materials from the recycling process, including REEs and nickel, and as such, does not ascribe any environmental impact credits to the outputs.

It is assumed that all products with economic value that are generated from the recycling process are sold in entirety at the prevailing price for those products, which are indicated in Table S10. For additional context and for comparison with literature estimates for primary and recycled production of relevant materials, we also calculate the environmental impacts on an output basis using a revenue-based economic allocation method. The revenue-based environmental impact e_{ij} in impact category i per kg of product j is calculated using Equation 16, where E_i is the environmental impact per 1000 kg of spent NiMH battery in impact category i, q_j is the amount of product j obtained per 1000 kg of spent NiMH battery, and p_j is the market price of product j.

$$e_{ij} = E_i \left(\frac{p_j}{\sum_j p_j q_j} \right) \quad \text{(Equation 16)}$$

Material and energy inputs to the recycling process shown in Table S11 were developed using the process flow shown in Figure S1. Life cycle inventories for material, energy, and transportation inputs are obtained from the Ecoinvent 3.5 database (Ecoinvent Center 2018) as global averages. Where data for exact or proprietary materials were unavailable, suitable substitutes were used. The average electricity mix for the recycling process is calculated as a recycling production-weighted average of the North American Electric Reliability Corporation (NERC) electricity mix for the locations of the recycling facilities. Recycling facility locations and their production quantities used to calculate this average mix are determined by the RELOG model. It should be noted that each NERC regional electricity mix process itself is an electricity generation-weighted average of various fossil, nuclear, and renewable electric power sources within that NERC region for the year 2018 based on U.S. EPA eGRID data (U.S. Environmental Protection Agency 2020), as shown in Table S17. Any water not contained in useful products (such as mixed hydroxides) is either disposed of as hazardous waste if present in the leach residue. Water generated from the neutralization of acidic solutions is assumed to be managed through ambient evaporation in ponds near the facility. As such, the process has no direct emissions to water.

Transportation environmental impacts from moving spent NiMH batteries from collection centers to storage and ultimately to the recycling facilities are calculated assuming a 16–32 tonne diesel-powered long-haul freight truck, and using the average distance traveled by 1000 kg of spent battery scrap over the analysis time horizon. This average value is calculated by dividing the total km of transportation distance from 2020 through 2050 by the tonnes of spent batteries collected during that same period as determined by the RELOG model and shown in Figure 5Error! Reference source not found.

We use the Cumulative Exergy Demand impact assessment method to understand abiotic material use impacts by different types of abiotic resources such as metals, non-metallic minerals, fossil resources, and bulk resources. We also use the ILCD 2011 impact assessment method to quantify climate change impacts and to evaluate abiotic depletion in a metric that allows comparison of our results with other literature estimates that have used ILCD 2011. The complete LCA results for both impact assessment methods are summarized in Tables S12–S15. The LCA modeling and analysis was conducted in the openLCA© software environment (Ciroth et al., 2020).

ADDITIONAL RESOURCES

Supplemental information is available for this paper.